

OCEAN5: the ECMWF Ocean Reanalysis System and its Real-Time analysis component

H. Zuo, M. A. Balmaseda, K. Mogensen,
and S. Tietsche

Research Department

August 2018

*This paper has not been published and should be regarded as an Internal Report from ECMWF.
Permission to quote from it should be obtained from the ECMWF.*



European Centre for Medium-Range Weather Forecasts
Europäisches Zentrum für mittelfristige Wettervorhersage
Centre européen pour les prévisions météorologiques à moyen terme

Series: ECMWF Technical Memoranda

A full list of ECMWF Publications can be found on our web site under:

<http://www.ecmwf.int/publications/>

Contact: library@ecmwf.int

©Copyright 2018

European Centre for Medium-Range Weather Forecasts
Shinfield Park, Reading, RG2 9AX, England

Literary and scientific copyrights belong to ECMWF and are reserved in all countries. This publication is not to be reprinted or translated in whole or in part without the written permission of the Director-General. Appropriate non-commercial use will normally be granted under the condition that reference is made to ECMWF.

The information within this publication is given in good faith and considered to be true, but ECMWF accepts no liability for error, omission and for loss or damage arising from its use.

Abstract

The ECMWF OCEAN5 system is a new global eddy-permitting ocean-sea ice ensemble reanalysis-analysis system. This Technical Memorandum gives a full description of the OCEAN5 system, with the focus on its Behind-Real-Time (BRT) component, the reanalysis product ORAS5. The OCEAN5 Real-Time (RT) component includes all upgrades developed for ORAS5 and runs daily using the latest observations and forcing fields from the operational Numerical Weather Prediction (NWP).

ORAS5 includes 5 ensemble members and covers from 1979 onwards. Compared to ORAS4, the ocean model resolution has been increased to an eddy-permitting resolution (0.25°) in the horizontal and a near-surface resolution of 1 m in the vertical. ORAS5 also includes a prognostic thermodynamic-dynamic sea-ice model with assimilation of sea-ice concentration data. Both observation data sets and forcing fields have been updated as well. An important novelty in ORAS5 is a generic ensemble generation scheme for perturbing both observations and forcing fields. Other upgrades include revisions to the ensemble-based spin-up and a-priori bias correction scheme. Assessment of ORAS5 and sensitivity experiments suggests that all system components contribute to an improved ocean analysis state, with directly assimilation of temperature and salinity in-situ data as the most influential term. Compared to ORAS4, ORAS5 also shows improved ocean climate variability in terms of Sea Surface Temperature (SST) and sea-level when verified against independent observation data sets. The SST biases in the Gulf Stream region remain large in ORAS5 though, which is associated with a misrepresentation of front positions and overshoot of the northward transport of the Gulf Stream.

1 Introduction

Ocean Reanalyses are reconstructions of ocean state using an ocean model integration constrained by atmospheric surface forcings, and ocean observations via a data assimilation method. Large scale bias correction is often applied too in order to remove spurious climate signals arising from the changing nature of the observing system; bias correction is also needed to avoid model drifts during periods with sparse observations in the distant past. The ocean model and data assimilation method are kept frozen during the production of the reanalysis. The primary function of the ocean reanalyses at ECMWF is to initialize the coupled re-forecast, and therefore a Real-Time (RT) extension of the reanalysis is critical for the timely production of operational forecasts. Consistency between the ocean reanalysis and RT analysis is crucial. This is obtained by keeping a tight link between the RT extension and the reanalysis.

Ocean Reanalyses with a Real-Time extension have been produced routinely at ECMWF since 2002, when the OCEAN2 system was implemented [Balmaseda, 2005] as integral part of the seasonal forecasting system. It was with the implementation of OCEAN3 [Balmaseda et al., 2008] that the ocean reanalysis was run independently of seasonal forecasts, since it was also used to initialize the extended range (re-)forecast; this was the first time that ocean reanalysis at ECMWF were used to monitor the ocean climate. OCEAN4 [Balmaseda et al., 2013] followed the same structure as OCEAN3, but it was a major upgrade: it was the first time that the NEMO ocean model was used at ECMWF, and the variational data assimilation NEMOVAR [Mogensen et al., 2012] was introduced.

OCEAN5 is the fifth generation of ocean reanalysis-analysis system at ECMWF. It comprises a Behind-Real-Time (BRT) component, that was used for production of Ocean ReAnalysis System 5 (ORAS5); and a Real-Time (RT) component, that is used for generating daily ocean analysis for NWP applications. The ORAS5 has been developed at ECMWF based on ORAP5 [Zuo et al., 2015], a prototype system which was developed within the EU funded research projects MyOcean and MyOcean2. The production of ORAS5 has then been funded by the Copernicus Climate Change Service (C3S). As a successor to ORAS4 [Balmaseda et al., 2013], ORAS5 benefits from many upgrades in both model and

data assimilation method, as well as in source/use of observation data sets. The ocean model resolution has been increased to 0.25° in the horizontal and 75 levels in the vertical, compared to 1° and 42 layers in ORAS4. ORAS5 also includes a prognostic thermodynamic-dynamic sea-ice model (LIM2, see Fichfet and Maqueda [1997]) with assimilation of sea-ice concentration data. Another important novelty in ORAS5 is the explicit inclusion of surface waves effects in the exchange of momentum and turbulent kinetic energy [Breivik et al., 2015]. The NEMOVAR data assimilation scheme has been updated with a new Rossby-radius-dependent spatial correlation length-scale [Zuo et al., 2015] and a new generic ensemble generation scheme which accounts for both representativeness errors in observation and structure/analysis errors in surface forcing [Zuo et al., 2017a]. ORAS5 is also consistent with the latest ECMWF atmospheric reanalysis-ERA5 [Hersbach and Dee, 2016], using the HadISST2 SST and the OSTIA sea-ice concentration to constrain its surface boundary conditions. Other innovative features include an ensemble-based a-priori bias correction scheme and the spin-up strategy, as well as revised observation quality control (QC) procedures. The OCEAN5-RT component includes all upgrades developed for ORAS5. It is initialized from ORAS5, and runs once a day to provide ocean and sea-ice initial conditions for all ECMWF coupled forecasting system.

The aim of this document is to describe ORAS5 as the ocean reanalyses component of the OCEAN5 system. Details of system upgrades after ORAP5 are discussed. This includes updates in the surface forcing (in Section 2.2), updates in surface/in-situ observation data sets and assimilations (in Section 2.3); updates in altimeter observation and assimilation (in Section 2.4); generation of the ensemble perturbations (in Section 2.5). The OCEAN5-RT analysis is presented in Section 2.6. Assessment of the ORAS5 performance has been carried out in Section 3.2 via diagnostics in observation space, and in Section 3.3 for selected ocean Essential Climate Variables (ECV).

2 The ORAS5 system

ORAS5 has been produced as the BRT component of the OCEAN5 system as a global eddy-permitting ocean ensemble reanalysis, covering the period from 1979 onwards. ORAS5 is an update of ORAP5. Here we give a brief overview of the model and methods used, with emphasis on the differences between ORAP5 and ORAS5 (See Table 1).

2.1 Ocean-sea ice model and data assimilation

ORAS5 uses the same ocean model, data assimilation, and spatial configuration as ORAP5 (Table 1). The NEMO ocean model version 3.4.1 [Madec, 2008] has been used for ORAS5 in a global configuration ORCA025.L75 [Bernard et al., 2006], a tripolar grid which allows eddy to be represented approximately between 50°S and 50°N [Penduff et al., 2010]. Model horizontal resolution is approximately 25 km in the tropics, and increases to 9 km in the Arctic. There are 75 vertical levels, with level spacing increasing from 1 m at the surface to 200 m in the deep ocean. NEMO is coupled to the Louvain-la-Neuve sea-ice model version 2 (LIM2, see Fichfet and Maqueda [1997]) implemented with the viscous-plastic (VP) rheology. The Wave effects introduced since ORAP5 [Breivik et al., 2015] were also implemented in ORAS5, with updated ocean mixing terms (TKE mixing in partial ice cover and revised wind enhanced mixing).

The reanalysis is conducted with NEMOVAR [Weaver et al., 2005, Mogensen et al., 2012] in its 3D-Var FGAT (First-Guess at Appropriate Time) configuration. NEMOVAR is used to assimilate subsurface temperature, salinity, sea-ice concentration (SIC) and sea-level anomalies (SLA), using a 5 day assimi-

Table 1: Overview of differences between ORAP5 and ORAS5 ocean reanalyses settings

	ORAP5	ORAS5
grids	~0.25°, 75 vertical levels	Same as ORAP5
model	NEMO 3.4, LIM2 ice model, wave effects	as ORAP5 + TKE mixing in partial ice cover + updated wave effects
forcing	ERA-Interim bulk formula + wave forcing	ERA-40 (before 1979) ERA-Interim (1979-2015) ECMWF NWP (2015-present) bulk formula + wave forcing
assimilation	NEMOVAR with revised correlation length-scales	as ORAP5 + stability check for bias correction + updated observation QC + revised parametrizations
bias corre.	adaptive bias correction scheme offline bias + online bias	as ORAP5 + ensemble estimation of offline bias
observations		
SST	Reynolds OIv2d [Reynolds et al., 2007] + OSTIA reprocessed + OSTIA operational	HadISST2 + OSTIA operational [Donlon et al., 2012]
T/S prof	EN3 with XBT/MBT correction [Wijffels et al., 2008]	EN4 with XBT/MBT correction [Gouretski and Reseghetti, 2010] + NRT
SLA	AVISO DT2010 [Dibarboure et al., 2011]	AVISO DT2014 [Pujol et al., 2016] with revised MDT + NRT
sea-ice	Same as SST	as ORAP5 + use OSTIA operational in 2008
period	1979-2013	1979-present
ensemble	1 member	5 members with perturbations in initial conditions, forcings and observations
spin-up	recursive spin-up 1979-1990 forced run 1975-1979 assimilation	recursive spin-up with 5 ensemble members 1958-1975 with different parameter choices 1975-1979 with ORAS5 parametrizations

tion window with a model time step of 1200 s. The observational information is also used via an adaptive bias correction scheme [Balmaseda et al., 2013], which will be explained in Section 2.3.

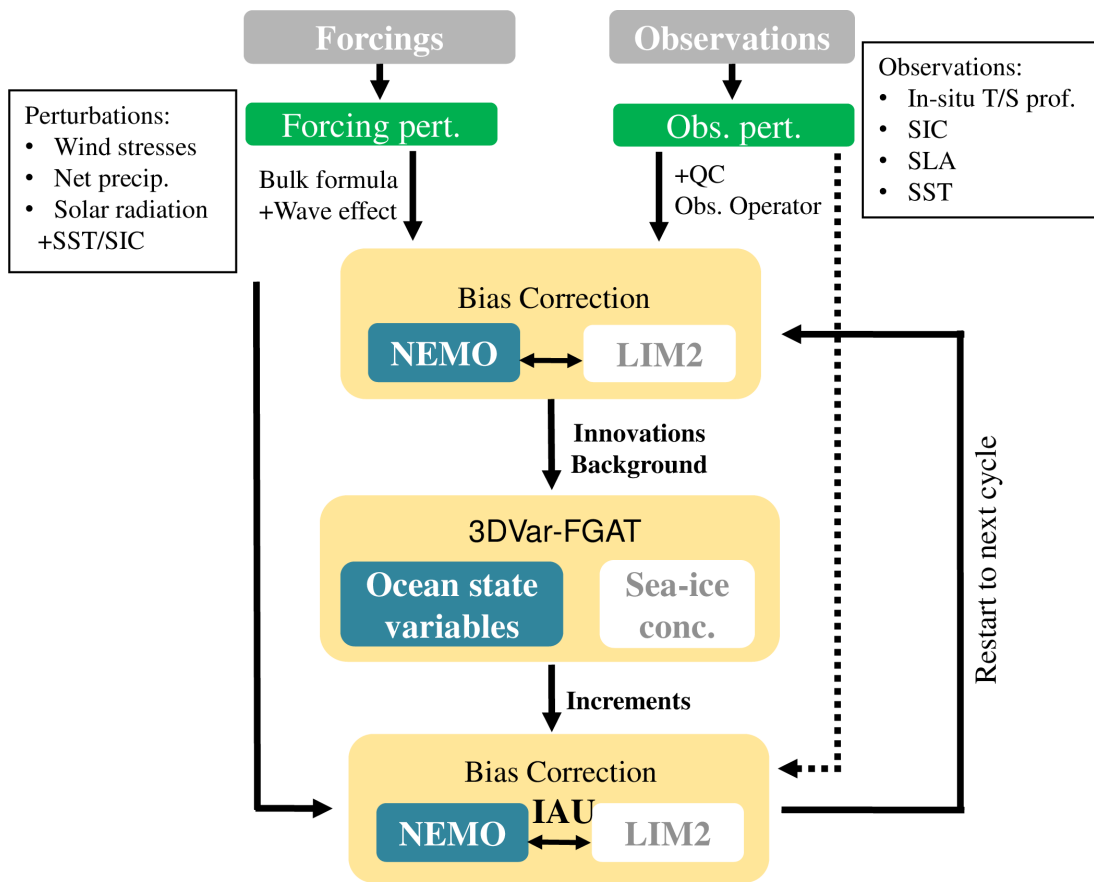


Figure 1: Schematic diagram of the ORAS5 system

A schematic diagram of the ORAS5 system can be found in Fig 1. The analysis cycle consists of one outer iteration of 3D-Var FGAT with observational QC and bias correction steps. In the first step (also called the first outer loop), the NEMO model is integrated forward and used for calculation of the model equivalent of each available observation at the time step closest to the observation time, after which the QC of the observations is performed. The quality-controlled observations and model equivalent background fields are passed to the so-called inner loop, where the 3D-Var FGAT method minimizes the linearized cost function to produce the assimilation increment. The increment is applied during a second forward integration of the model (the second outer loop) using the incremental analysis updates method with constant weights (IAU; Bloom et al. [1996]). Both SIC and other observations are assimilated using a 5-day assimilation cycle in ORAS5 and share the outer loop model integrations.

As in ORAP5, assimilation of SIC data is also included in ORAS5. The background state of ocean and sea ice is produced from a coupled NEMO-LIM2 run, but the minimization of the SIC cost function is separated from the minimization of the cost function for all other ocean state variables. The separation of the sea-ice minimization assumes that there are no covariances between SIC and other variables. Variables which are physically related are divided into balanced and unbalanced components. The balanced components are linearly dependent (related by the multi-variate relationships), while the unbalanced components are independent and uncorrelated with other variables. The ORAS5 balance relations are the same as for ORAS4 [Mogensen et al., 2012] and ORAP5. The observation and background errors specifications are the same as in ORAP5 [Zuo et al., 2015], except for sea level (see Section 2.4).

2.2 Model initialization and forcing fields

2.2.1 Initialization

As for the previous ocean reanalysis system ORAS4, perturbing the ocean initial conditions at the beginning of the reanalysis period is considered paramount. In ORAS4 different initial states in 1958 were given by sampling a 20 year ocean integration. ORAS5 had a longer spin-up using reanalyses for the period 1958-1979, conducted using either ERA40 [Uppala et al., 2005] or ERA20C [Poli et al., 2016] forcing and assimilating in-situ data. ORAS5 starts in 1979, so it is in principle possible to have initial conditions representative of that given date. A series of ocean reanalyses assimilating in-situ profiles using different surface forcing, data sets and parameters was conducted from the period 1958 to 1975 (Table 2a), as an attempt to account for the uncertainty of ocean state at a given point in time. The interested reader is referred to Table 5 in the Appendix for experiment IDs of these pre-production experiments. This approach gives a set of 5 initial conditions (INI1-5) to start each of the ensemble member of ORAS5, thus generating the ORAS5 initial perturbations. The control member of ORAS5 (hereafter ORAS5.1) was initialized from INI1 with a similar configuration to ORAP5, and is unperturbed: neither the forcing fields nor the observations perturbations are applied (see Section 2.5 for details). A second spin-up from 1975 to 1979 was then conducted with the same settings as used for ORAS5, and the integrations are then continued after 1979. The impact of the initial perturbations is illustrated in Fig. 2, which shows the evolution of the global ocean heat content (OHC) from the 5 spin-up ocean reanalyses listed in Table 2a, and ORAS5 with its 5 ensemble members.

The initial uncertainty of ORAS5 OHC is illustrated by OHC spread (here we define the spread as the maximum value minus minimum value in OHC, taking into account all ORAS5 ensemble members at a given time) in Fig. 2. The initial spread inherited from the 5 spin-up remains high especially for the first 5 years between 1975-1979. There is a constant reduction of OHC for all members during 1975-1982, with rapid cooling for two warm members initialized from INI4 and INI5. This OHC spread reduces gradually and reaches a relatively stable state after 2000, suggesting a robust uncertainty maintained by the other components of the perturbation scheme (See Section 2.5).

2.2.2 Forcing, SST and SIC

Forcing fields for ORAS5 are derived from the atmospheric reanalysis ERA-Interim [Dee et al., 2011] until 2015, and from the ECMWF operational NWP thereafter (see Fig. 3), using revised CORE bulk formulas [Large and Yeager, 2009] that include the impact of surface waves on the exchange of momentum and turbulent kinetic energy [Breivik et al., 2015]. Compared to ORAP5, the wind enhanced mixing due to surface waves is updated with a revised spatial distribution scheme. In addition, sea surface temperature (SST), sea surface salinity (SSS), global mean sea level trends and climatological variations of the ocean mass are used to modify the surface fluxes of heat and freshwater.

SST is assimilated in ORAS5 by modifying the surface non-solar total heat flux using the product of a globally uniform restoration term of $-200 \text{ W m}^{-2} \text{ K}^{-1}$ and the difference between modelled and observed SST (see Haney [1971]). The effect of this restoration can be illustrated as follows: assuming a constant mismatch to observations of 1 K within a well mixed upper 50 m water, the relaxation term will restore the water temperature in this mixed layer by 1 K in about 12 days. The numerical value is unchanged from previous ECMWF ocean reanalyses; the original choice was motivated to keep SST errors within 0.2 K in the global ocean. The same value is used in other ocean reanalysis systems with similar horizontal resolution as ORAS5 [Masina et al., 2017]. However, given that ORAS5 has finer vertical resolution,

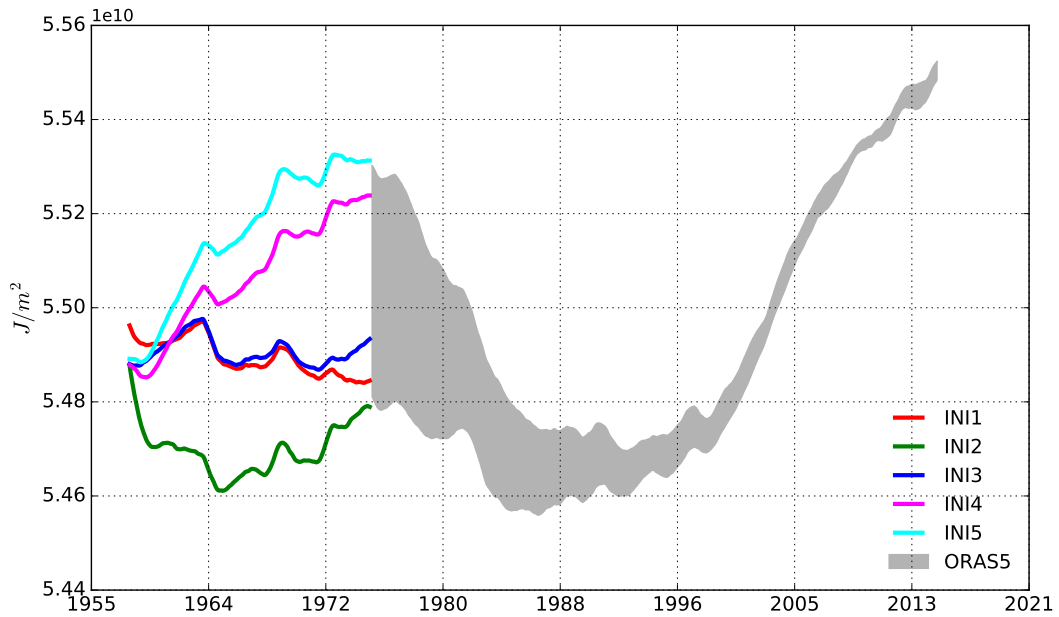


Figure 2: Time series of global ocean heat content (in 10^{10} Jm^{-2}) integrated for the whole water column, from 5 spin-up runs (INI1-5, 1958-1979) and ORAS5 from 1975 onwards. The shaded areas encompass the spread of all ORAS5 ensemble members. A 12-month running mean has been applied.

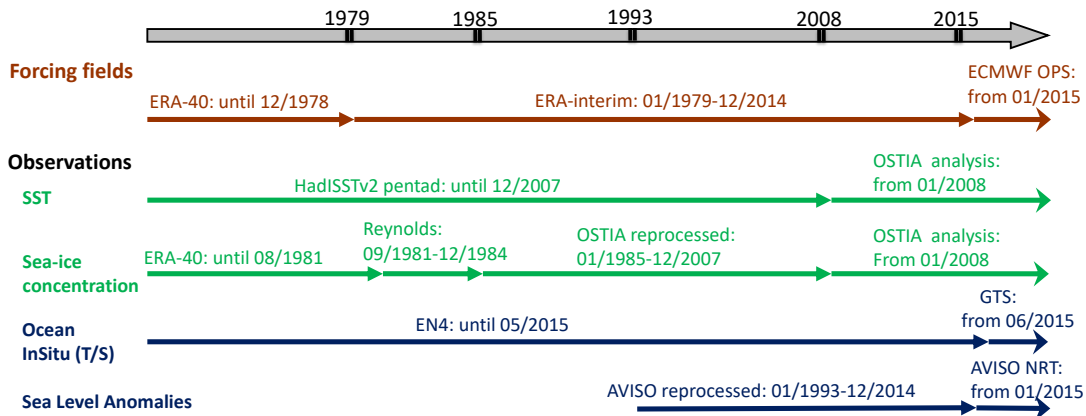


Figure 3: Time line of changes to the reanalysis forcing and assimilation data sets for ORAS5

this term may need revision. Besides, it has also been found that ocean circulation in climate model is sensitive to the strength of SST restoration [Servonnat et al., 2014]. More discussion of SST nudging and

Table 2: Summary of ensemble pre-production runs for generating ORAS5 initial conditions and off-line bias correction terms. All carried out in ORCA025.L75 configuration.

(a) Ensemble of ORAS5 initial conditions

Name	Initialization	Forcing	SST/SIC	In-situ	Sali. Capping	ϕ_c
INI1	ORAP5-1990	ERA40	ERA40	EN3	No	10°
INI2	ORAP5-1980	ERA20C	HadISST2	EN4	No	10°
INI3	INI1-1970	ERA40	ERA40	EN4	Yes	10°
INI4	INI1-1970	ERA40	HadISST2	EN4	Yes	2°
INI5	INI1-1970	ERA40	HadISST2	EN4	No	10°

ϕ_c are parameters defining the latitudinal Gaussian decay of online bias correction, see Eq. 6 and 7 in Zuo et al. [2015].

(b) Ensemble of ORAS5 offline bias correction

Name	SST	SIC	Vert. Deri. Estim.	H. Thin. Dist.	σ_T^{do}
BIAS1	HadISST2	HadISST2	finite differences	100km	0.07
BIAS2	HadISST2	HadISST2	cubic spline	100km	0.07
BIAS3	OSTIA	OSTIA	cubic spline	25km	0.07
BIAS4	OSTIA	OSTIA	cubic spline	25km	0.098
BIAS5	HadISST2	OSTIA	cubic spline	25km	0.098

σ_T^{do} is the minimum temperature observation error standard deviation at deep ocean, see Zuo et al. [2015].

All BIAS runs assimilated EN4 data but without SLA assimilation.

associated impact on ocean state can be found in Section 3.3.1. A similar global uniformed SSS restoration term of -33.3 mm/day to climatology has been applied by adding a term to the surface freshwater fluxes equation.

Temporal consistency in the SST analysis product employed is important for both ocean and atmospheric reanalysis. Hirahara et al. [2016] found that the OSTIA SST reanalysis product has a noticeably different global mean with respect to its homonymous real-time product; they recommended to use SST from [Titchner and Rayner, 2014] in combination with the real-time OSTIA for production of the atmospheric reanalysis ERA5. HadISST2.1 is a new pentad SST product with a spatial resolution of 0.25° resulting from the EU FP7 project ERA-CLIM2. The bias correction and data homogenization in this product is superior to its predecessor HadSST3 [Kennedy et al., 2011a,b], and more importantly, the resulting SST are consistent with those delivered operationally by OSTIA [Donlon et al., 2012]. ORAS5 has adopted the same SST as ERA5. Therefore, SST in ORAS5 prior to 2008 comes HadISST2.1, and from operational OSTIA thereafter.

The SIC data assimilated in ORAS5 comes from the OSTIA reanalysis before 2008. This is the same as in ORAP5. Sea-ice data in HadISST2.1 includes both re-processed sea-ice concentration data from the EUMETSAT Ocean and Sea Ice Satellite Application Facilities (OSI-SAF) and polar ice charts data from National Ice Center (NIC). SIC in HadISST2.1 is calibrated against NIC sea-ice charts in order to ensure consistency with chart analyses prior to the satellite era. However, sea-ice concentration in sea-ice charts has large uncertainties itself [Karvonen et al., 2015]. Moreover, some sea-ice charts are biased towards high SIC, because they are made to warn marine users of hazardous ice conditions, and the ice analysis will always assign higher SIC if there is any doubt in order to allow for a safety margin. As a result, sea-ice concentration in the HadISST2.1 data is substantially higher than in the OSI-SAF data [Titchner and Rayner, 2014] and OSTIA analysis .

In order to assess the impact of assimilating different SST and SIC products in our system, sensitivity experiments have been carried out at ORCA1.L42 resolution (approximately 1° at tropics with 42 vertical levels) with ORAP5-equivalent Low-Resolution configuration (hereafter referred to as OP5-LR). SST and SIC data used in these experiments are listed in Table 3a, together with the experiment names. The reader is referred to Table 6 in Appendix for experiment IDs of these experiments. Global mean SST from these experiments are shown in Fig. 4, together with the SST analysis products that were assimilated. For verification, the latest European Space Agency Surface Temperature Climate Change Initiative (ESA SST CCI) multi-year SST record [Merchant et al., 2014] (version 1.1) is also included here as a reference. This data set is generated from satellite observations only and is independent from in situ observations.

Despite the discrepancy in the early period, HadISST2 and OSTIA SST analyses are very similar after 2008, suggesting that HadISST2 is more consistent with the operational OSTIA SST product than the OSTIA reanalysis SST itself, as already pointed out by Hirahara et al. [2016]. OSTIA reanalysis SST is systematically colder than both HadISST2 and ESA CCI SST before 2008, by approximately 0.1°C and 0.16°C in the global mean, respectively. Unlike HadISST2 and OSTIA, both of which define SST as the night-time temperature, ESA CCI SST are defined as the daily-mean temperature at 0.2 m depth, and thus provides the warmest SST among these three products. Time-series of global mean SST from ASM-HadI and ASM-HadI-OST are almost indistinguishable from each other, or from HadISST2 itself. ASM-OST, on the other hand, generates a global mean SST which lies in-between OSTIA reanalysis and HadISST2 SST. This result indicates that assimilated near-surface in-situ observations agree better with HadISST2 SST than with OSTIA SST. This lack of consistency between near-surface in-situ observations and OSTIA reanalysis, and between operational OSTIA SST and OSTIA reanalysis, determined the final choice of SST product for ORAS5.

The above experiments were also used to inform the choice of the SIC data set. Departure of sea-ice thickness (SIT) from the three sensitivity experiments (Table 3a) against laser altimeter freeboard measurements from ICESat [Kwok et al., 2009] (data downloaded from <http://nsidc.org/data/nsidc-0393>) for October 2007 are shown in Fig. 5. Among the three, ASM-HadI-OST clearly shows the smallest SIT discrepancy, especially for the thick ice in the Beaufort Gyre and at the north coast of Greenland and the Canadian Archipelago. Assimilating HadISST2 SIC data results in profoundly overestimated SIT in ASM-HadI as verified against ICESat observations. This leads to unrealistic sea-ice conditions in both the Arctic and the Antarctic in ASM-HadI (not shown). As a result, we chose to use the OSTIA reanalysis SIC in ORAS5 until 2008, together with SST observation from HadISST2.

Table 3: Summary of sensitivity experiments carried out to inform the choice of the final ORAS5 configuration. All experiments are carried out at ORCA1.L42 resolution and in OP5-LR configuration unless specified otherwise.

(a) Sensitivity experiments to inform the choice of SST/SIC observation products

Name	SST	SIC
ASM-HadI	HadISST2	HadISST2
ASM-OST	OSTIA	OSTIA
ASM-HadI-OST	HadISST2	OSTIA

(b) Sensitivity experiments to inform the choice of in-situ observation data set

Name	In-situ data set
EXP3	EN3 data set with bias correction from Wijffels et al. [2008]
EXP4	EN4 data set with bias correction from Gouretski and Reseghetti [2010]

(c) Sensitivity experiments to inform the configuration of observation quality control

Name	QC pair check
PC-OFF	QC without a temperature/salinity pair check
PC-ON	QC with a temperature/salinity pair check

(d) Sensitivity experiments to inform configuration of the bias correction scheme

Name	Bias correction capping	N_{min}^2
NoCap	Without capping the salinity bias correction term	N/A
CP10	With capping the salinity bias correction term	$1e^{-10}$

N_{min}^2 is the minimum value of the squared buoyancy frequency
Both experiments assimilate EN4 in-situ observations

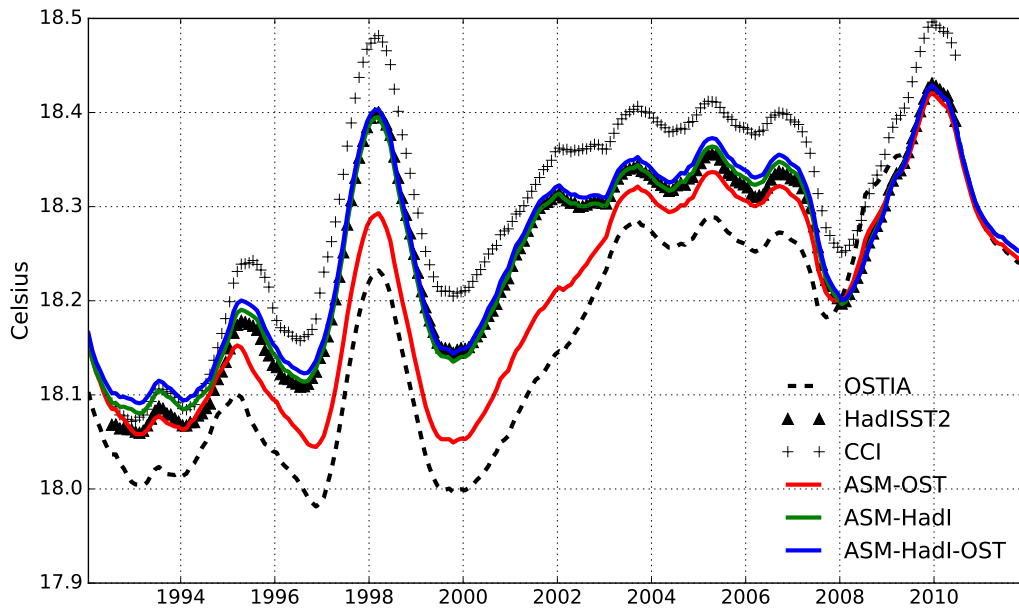


Figure 4: Time series of global mean SST (°C) from ocean reanalyses when assimilating different SST and SIC analysis products. A 12-month running mean filter has been applied.

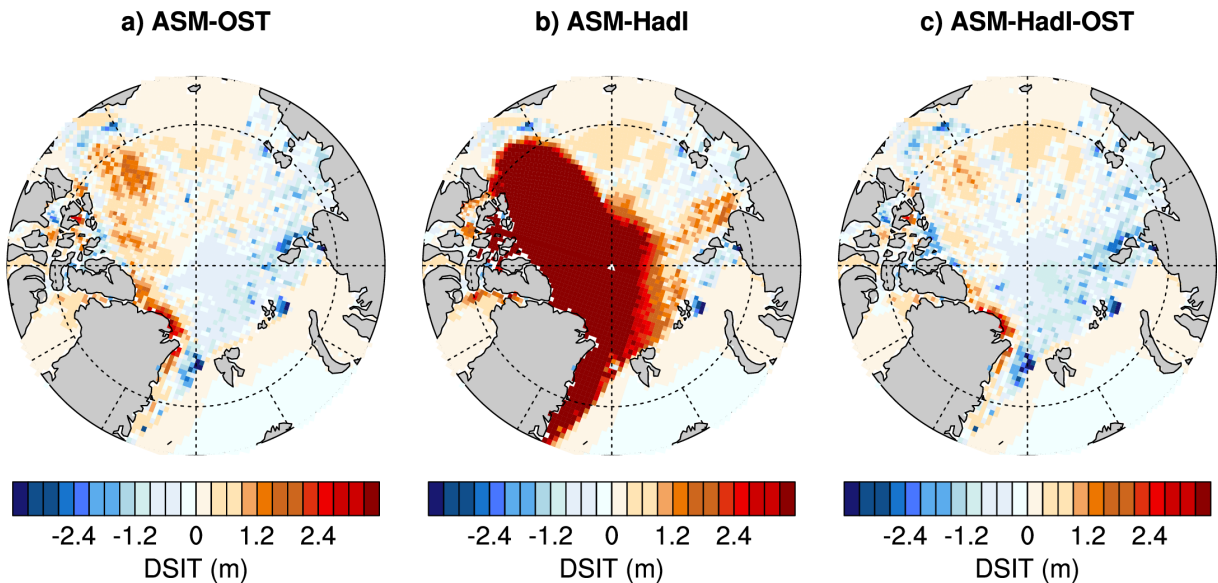


Figure 5: Departure of sea-ice thickness in meters for (a) ASM-OST, (b) ASM-HadI and (c) ASM-HadI-OST. The departure is computed with respect to ICESat observations for October 2007.

2.3 Assimilation of in-situ observations

2.3.1 Update in observational data set

The in-situ temperature and salinity (T/S) profiles in ORAS5 come from the recently released quality controlled data set EN4 [Good et al., 2013] with Expendable BathyThermograph (XBT) and Mechanical

bathythermograph (MBT) depth corrections from [Gouretski and Reseghetti \[2010\]](#) until May 2015. EN4 is a re-processed observational data set with globally quality-controlled ocean T/S profiles. It includes all conventional oceanic observations (Argo, XBT/MBT, Conductivity-Temperature-Depth (CTD), moored buoys, ship and mammal-based measurements). Data from the Arctic Synoptic Basin Wide Oceanography (ASBO) project was also included in EN4 with the aim to improve data coverage in the Arctic. Compared to its predecessor EN3 (used in ORAS4 and ORAP5), EN4 has increased vertical resolution, additional QC and duplication check, and extends farther back in time. For the latest years, EN4 also contains a more complete and cleaned record of the Argo data, with bias-corrected data whenever possible.

The EN4 version 4.0.2 (EN402) with bias corrections from [Gouretski and Reseghetti \[2010\]](#) is used from 1975 onwards, and switches to version 4.1.1 (EN411) with the same bias correction for the years 2014 and 2015. After May 2015, ORAS5 starts using the operational data from the Global Telecommunications System (GTS), which consists of data received in near-real-time at ECMWF.

The new EN4 data set has been evaluated against the EN3 data set using twin experiments carried out in the OP5-LR configuration at ORCA1.L42 resolution (see [Table 3b](#)). Twin experiments comprise a reference run EXP3 that assimilates EN3 data, and another run EXP4 that assimilates EN4 data but are otherwise identical. Differences between EXP3 and EXP4 in temperature and salinity averaged over 2005 to 2012 can be found in [Fig.6](#).

In general, the switch from EN3 to EN4 has a neutral impact on the ocean reanalysis results. Differences in the upper 300 m are more pronounced compared to the deep ocean (see [Fig.6](#)), and are directly related to discrepancies between the EN3 and EN4 data sets (not shown). EXP3 and EXP4 also share similar ocean circulation, except for the sub-polar gyre of the North Atlantic Ocean, where the North Atlantic water between 1000 and 2000 m is slightly warmer in EXP4. Large discrepancies in the Arctic domain are noticeable in [Fig. 7](#). Large salinity differences (± 0.2 psu) appear near the Greenland coast, at the edge of East Siberian Sea and across the Baffin Bay. These are also associated with corresponding differences between EN3 and EN4, which suggests that the data assimilation has directly transferred the salinity differences from the observations to the reanalyses. Spatial patterns of temperature and salinity differences in the Arctic are with similar scale (approximately 500 km). Considering the sparse in-situ observations available in the Arctic domain, those differences may be induced by the model forward propagation of the in-situ information.

The Arctic is a difficult region for ocean data assimilation, owing to sparse data coverage both from in-situ profiles and satellite surface observations. Thanks to the improved observation coverage in EN4, with an Arctic total observation number almost doubled after 2005 compared to EN3, ORAS5 is expected to provide a better estimation of the Arctic ocean state, particularly for the latest period. This can be demonstrated by verifying against independent in-situ observations. A group of CTD mooring arrays in the Barents Sea has been withdrawn from data assimilation in EXP3 and EXP4. It is the only long-term observation array available with a large enough spatial coverage in the Arctic area. Bias and root-mean-square error (RMSE) statistics of the model background departures from CTD observations are presented in [Fig. 8](#). Both temperature and salinity RMSE are reduced after switching the assimilated data from EN3 to EN4, suggesting an improved performance of EXP4 in this region.

2.3.2 *Update in observation quality control*

All input observation are subjected to a global quality control procedures similar to those employed in EN4. Among these are checks on duplication, background, stability, bathymetry, and using the Argo grey

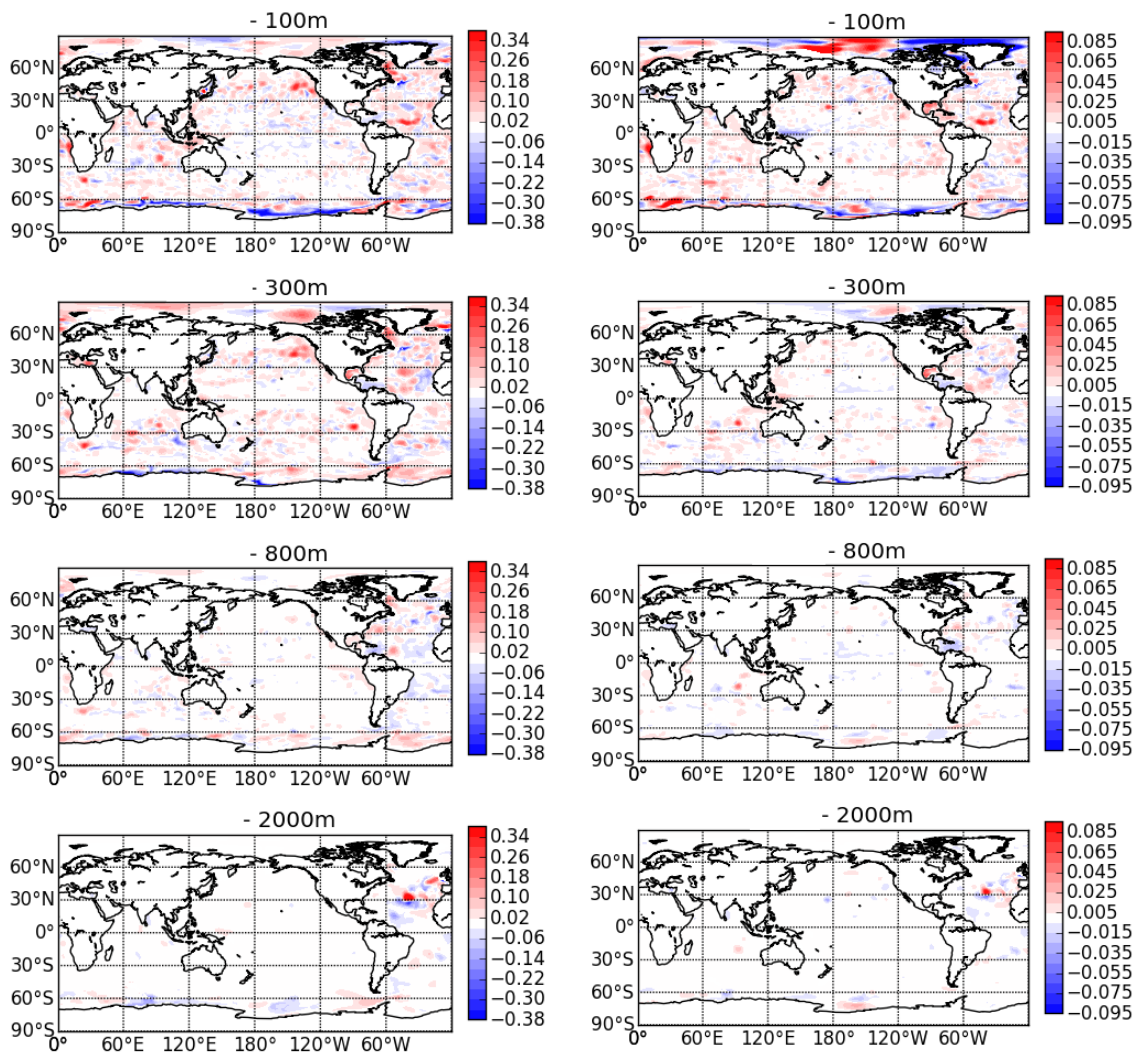


Figure 6: Differences in (left) temperature (K) and (right) salinity (psu) between EXP4 and EXP3. These are similar to the differences between EN4 and EN3 in-situ observations (not shown). Statistics are computed over the period 2005–2012 at different depths (100, 300, 800 and 2000 m).

list (from ftp://ftp.ifremer.fr/ifremer/argo/etc/ar_grey-list/). In addition, a new temperature–salinity pair check has been introduced in ORAS5, in which salinity observation will be rejected whenever the corresponding temperature observation from the same profile at the same depth level has either been rejected or does not exist. This pair check has been designed to avoid assimilating salinity observation alone when the temperature observation is not available. Temperature is the primary variable in the multivariate balance operator [Weaver et al., 2005] of NEMOVAR, therefore the pair check reduces the risk of introducing spurious vertical convection through data assimilation. This is important, for instance in the North Atlantic Ocean where the ocean data assimilation system is sensitive to the vertical structure of the temperature and salinity observation profile [Zuo et al., 2017a].

The pair check was tested using twin experiments (see Table 3c) in the OP5-LR configuration. The twin experiments comprise reference experiment without the T/S pair check (PC-OFF), and an otherwise identical experiment except that uses the pair check (PC-ON). Figures 9a,b highlight an inverse temper-

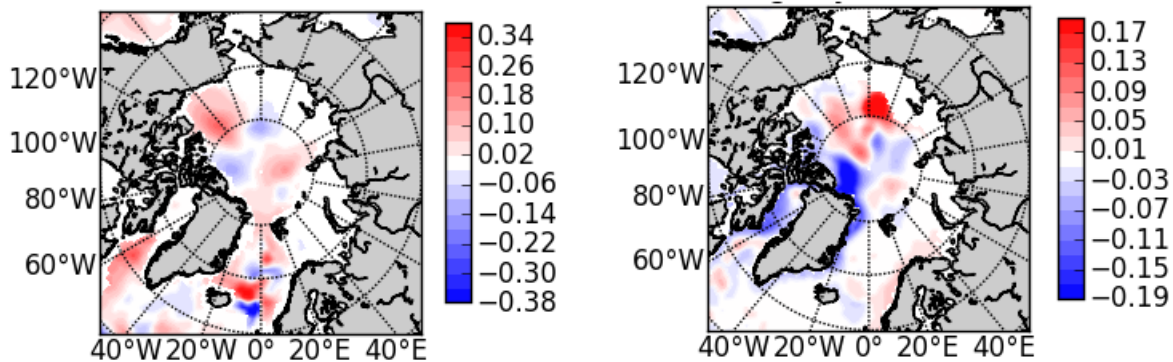


Figure 7: Differences in (left) temperature (K) and (right) salinity (psu) between EXP4 and EXP3 (same as Fig. 6 but displayed in a northern polar stereographic projection). Departures are computed as EXP4 minus EXP3 at 100 m depth and averaged between 2005-2012.

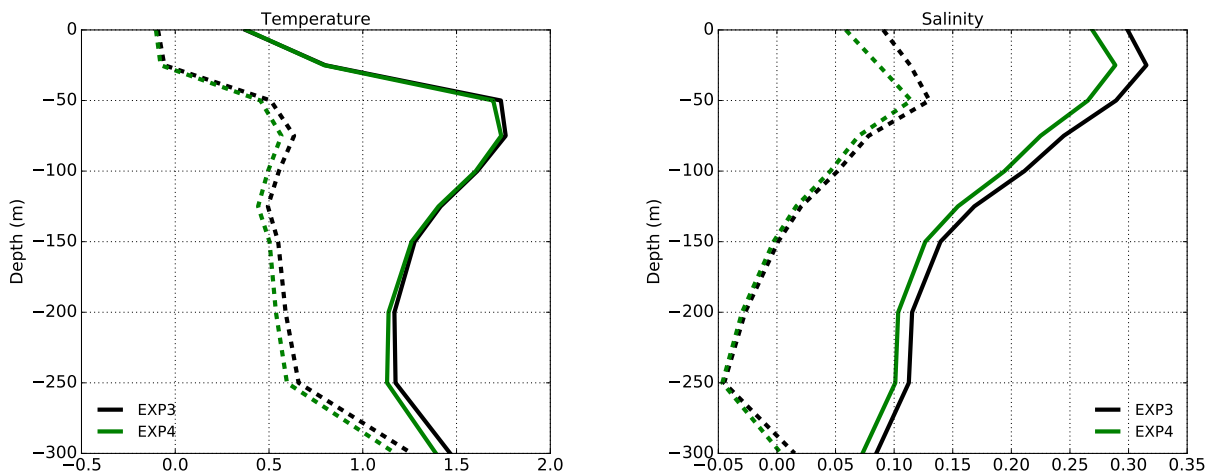


Figure 8: Profiles of model bias (dashed lines) and RMSE (solid lines) for (left) temperature (K) and (right) salinity (psu) for the upper 300 m. Statistics are calculated using the misfit of the model background value from (black) EXP3 and (red) EXP4 with respect to CTD profiles in the Barents Sea and for September 2009.

ature bias pattern in the eastern North Atlantic Ocean in PC-OFF, with cold bias up to 0.8 K at 1500 m and a warm bias of ~ 1 K at 2000 m. This was improved in PC-ON as shown in Figures 9c,d with a small compensating temperature difference defined as PC-ON minus PC-OFF, which also leads to reduced RMSE in PC-ON (not shown) between 1000–2000 m.

2.3.3 Update in the bias correction scheme

A similar multi-scale bias correction scheme as described in [Balmaseda et al. \[2013\]](#) has been implemented in ORAS5 to correct temperature/salinity biases in the extra-tropical regions. A pressure correction for the tropical regions has been implemented as well in this bias correction scheme. Compared to

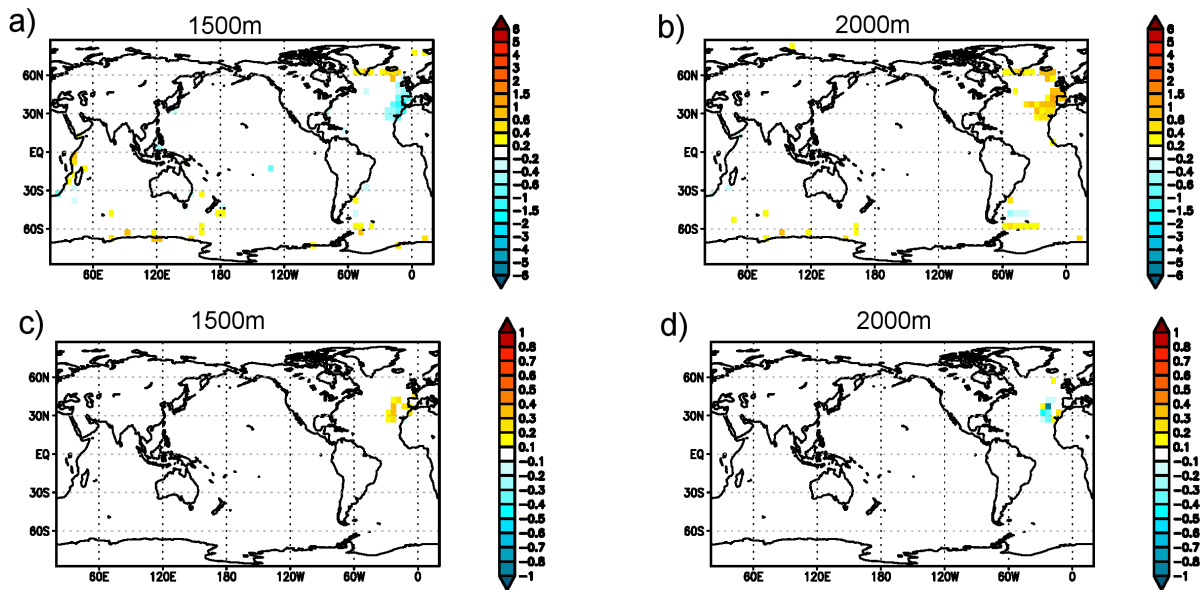


Figure 9: (a,b) PC-OFF mean temperature biases in K with respect to observations at (a) 1500 m and (b) 2000 m; (c,d) PC-ON temperature departures in K from PC-OFF at (c) 1500 m and (d) 2000 m. Statistics are computed based on September data over the period 2005–2010, after binning and averaging the observation-space departures over $5^\circ \times 5^\circ$ latitude/longitude boxes. The reader should note that the scale in (a,b) is 6 times larger than in (c,d).

ORAP5, the ORAS5 bias correction scheme includes two major upgrades. First, the a-priori bias (offline bias) in ORAS5 has been estimated using an ensemble of five realizations of assimilation runs (only temperature and salinity) during the Argo period (2003–2012) with different forcing and model parameters (See Table. 2b). The equivalent term in ORAP5 was estimated from a single realization of reanalysis from a different period (2000–2009). The ensemble approach allows uncertainties of model errors to be estimated, and could provide, in some regions, a more robust estimation of the model error. In ORAS5 only the ensemble mean of a-priori biases estimated from these 5 runs (BIAS1-5) was used to account for seasonal variations of the model errors.

Maps of the annual-mean offline bias correction applied in the three reanalyses ORAS4, ORAP5 and ORAS5 are shown in Fig. 10 for temperature and salinity, averaged over 300–700 m. In both ORAP5 and ORAS5, both temperature and salinity bias terms show much finer structure than in ORAS4, with sharp frontal structure along the northern edge of the Antarctic Circumpolar Current and along the Western Boundary Currents. Both ORAP5 and ORAS5 show very similar bias pattern in general, suggesting common model or forcing errors. However, bias terms in ORAS5 are clearly weaker than in ORAP5 almost everywhere in the global ocean, and especially for the Tropics. These reduced bias terms in ORAS5 are likely associated with (a) reduced model error due to an updated mixing scheme which accounts for enhanced mixing due to a flux of turbulent kinetic energy from breaking waves; (b) the new EN4 data set assimilated in the ORAS5 pre-production runs; (c) the difference in climatological period between ORAS5 and ORAP5 offline bias terms. Uncertainty of offline bias in ORAS5 derived from ensemble spread from the above 5 runs (BIAS1-5) is shown in Fig. 11. This kind of information is not yet utilized in the ORAS5 system. In future, use of this information should be exploited, e.g. for specifying the model background error matrix \mathbf{B} .

Furthermore, a stability check was introduced in the ORAS5 bias correction that caps the minimum value

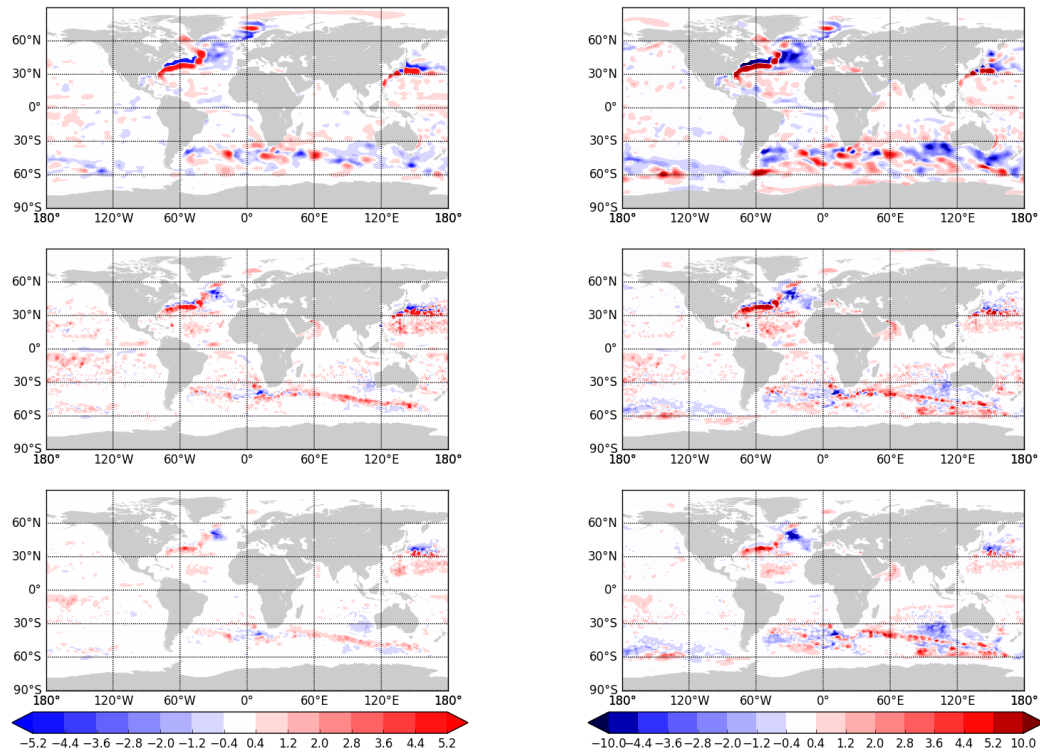


Figure 10: Offline bias correction term averaged over 300–700 m for (left) temperature (units are 0.01 K per 10 days) and (right) salinity (units are 0.001 psu per 10 days) applied in (top) ORAS4, (middle) ORAP5 and (bottom) ORAS5.

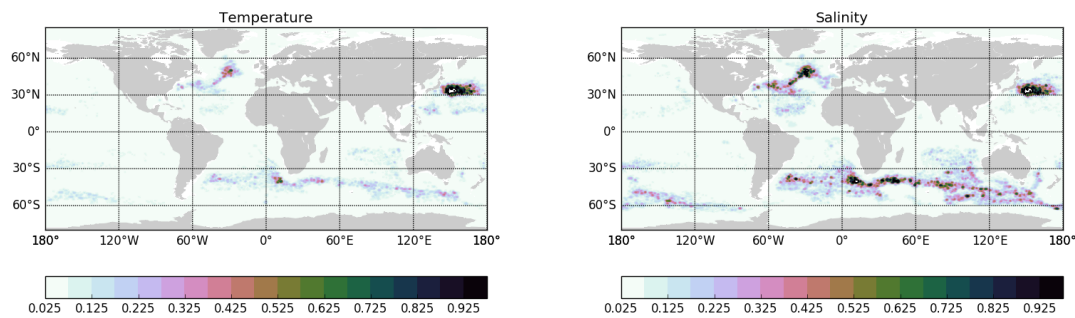


Figure 11: Ensemble spread of offline bias averaged over 300–700 m for (left) temperature (units are 0.01 K per 10 days) and (right) salinity (units are 0.001 psu per 10 days). Ensemble spread is defined as standard deviation of the 5 pre-production runs (see Table 2b).

of salinity bias correction term to prevent static instability. We define a minimum value for the squared buoyancy frequency as N_{min}^2 . In every model grid cell where N^2 as defined by the model background potential density profile (ρ_σ) is close to static instability ($N^2 \leq N_{min}^2$, $N_{min}^2 = 1e^{-10}$), we modify the salinity bias to ensure that δN^2 due to total bias (both temperature and salinity) is 0. In this way, the

salinity bias correction is prevented from introducing instability in the water column, which could otherwise induce spurious vertical convection, thought to be the cause of large reanalysis biases in regions around the Mediterranean outflow waters in the Northern Atlantic Ocean [Zuo et al., 2017b].

Results of model fit-to-observation errors from a set of twin assimilation experiments testing the impact of the bias capping can be found in Fig. 12. The twin experiments were set up in the OP5-LR configuration – but assimilating EN4 data set instead of EN3 (Table 3d). The reference run (NoCap) does not activate salinity bias capping, while the other run (CP10) adds salinity bias capping and has otherwise exactly the same configuration. Both temperature and salinity RMSE profiles of NoCap show a local maximum at 1000 m, which is associated with the spurious convection between 1000 and 2000 m due to warm and salty Mediterranean outflow. The new salinity bias capping in CP10 successfully reduces bias and RMSE for both temperature and salinity at this depth range. As a result, CP10 also exhibits improved sea level correlation with altimeter data (not shown) compared to NoCap.

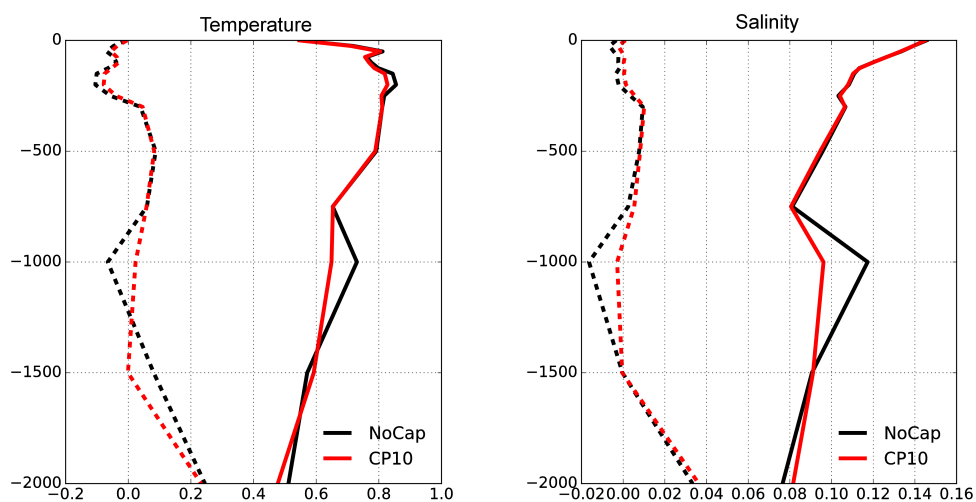


Figure 12: Profiles of model mean bias (dashed lines) and RMSE (solid lines) for (left) temperature in K and (right) salinity in psu. Statistics are calculated using the model background value from NoCap (in black) and CP10 (in red), with respect to the quality-controlled EN4 data set, after averaging over the 1996-2011 period and the eastern North Atlantic Ocean.

2.4 Assimilation of satellite altimeter sea-level anomalies

The sea-level anomaly (SLA) observations produced by AVISO (Archiving Validation and Interpretation of Satellite Oceanographic data) DUACS (Data Unification and Altimeter Combination System) has been updated to the latest version DT2014 [Pujol et al., 2016] in ORAS5 for both filtered along-track and gridded SLA data. The AVISO DT2014 data set has received a series of major upgrades since the previous version DT2010 [Dibarboure et al., 2011] that has been used in ORAS4 and ORAP5 reanalyses. These upgrades include, among others, a new 20-year altimeter reference period (1993–2012) instead of the previous 7-year reference period, additional satellite missions, use of up-to-date altimeter standards and geophysical corrections. The increased spatial resolution (14 km in low latitudes) of the DT2014 filtered along-track SLA data also results in improved meso-scale representation compared to DT2010.

A superob scheme has been implemented in ORAS4 as a method to account for observation representa-

tiveness errors from along-track SLA data, by constructing reduced grids for observation superobbing. This scheme has been updated in ORAS5 to include a stratified random sampling method [Zuo et al., 2017a]. Other parts of the scheme, e.g. a reduced-grid construction and a method for diagnosing observation error standard deviations (OBE STD) [Mogensen et al., 2012], remain unchanged. Despite that, the reduced grids used for observation pre-processing (typical 1° by 1° in latitude/longitude) are the same between ORAS4 and ORAS5, the increased resolution in DT2014 results in more SLA observations falling within each reduced grid than when using DT2010. Another important change in ORAS5 w.r.t. ORAS4 is that thinning is now done by stratified random sampling instead of creating superobbing SLA observations. As a result, ORAS5 ingests SLA observations with increased local variability but reduced OBE STD (by approximately 20% in the Tropics). ORAS5 also assimilates more along-track SLA data whenever newly available satellite missions (i.e. GeoSat Follow-On, HaiYang-2A, Topex New, Jason-1 Geodetic, Jason-1 New, Saral/AltiKa) are included in DT2014.

A reference mean dynamic topography (MDT) is required in order to assimilate SLA along-track data in an ocean general circulation model. This is necessary in order to compute model equivalents of observed SLA fields to construct innovations. In ORAS5, we compute the MDT by following the same strategy as in ORAP5, except that the previous assimilation run which only assimilates temperature and salinity data was produced using two parallel streams instead of one sequential integration. This was done to accelerate the process of computing the MDT, since multi-year ocean reanalyses with ORCA025 have a slow production rate. The MDT was then computed by averaging model sea-surface height over a reference period 1996–2012 and adding a term to correct biases introduced by using a reference period that is different from the DT2014 data set (see Zuo et al. [2015]). Such a pre-calculation of model-consistent MDT could be very expensive when used with a high resolution ocean general circulation model and/or a coupled data assimilation system. As an attempt to avoid this expensive step, assimilation of sea-surface height (SSH) with geoid information instead of using a reference MDT should be explored in the future.

The Global Mean Sea Level (GMSL) in ORAS5 was constrained using the same method as in ORAP5. The method uses a GRACE-derived climatology to constrain mass variation before 1993, and assimilates altimeter-derived GMSL after 1993. The GMSL was derived from observation, firstly using reprocessed DT2014 gridded SLA data up to 2014, then using AVISO NRT gridded SLA from 2015 onwards. A systematic offset of GMSL between these two data sets is expected due to data delay in the NRT product, and due to slightly different data processing methods (e.g. multi-mission mapping method). This has to be dealt with in order to avoid introducing spurious GMSL drift in the system. Assuming that sources of error do not change over time, this GMSL offset between delayed and NRT gridded SLA products can be derived using GMSL difference averaged over their overlapping period. In practice, the maximum overlapping period (from May 2014 to November 2014) at the time of ORAS5 production was used for computing this mean GMSL offset. This value was then added for bias correction of GMSL derived from NRT data from 2015 onwards. However, it means that this procedure needs to be repeated in the ocean analysis system whenever the observation process stream changes in NRT SLA production.

ORAS5 uses the same specification of SSH background error (BGE) and OBE as ORAP5 (see details in Zuo et al. [2015]). We tested different SSH OBE standard deviation as an attempt to account for increased spatial resolution in the DT2014 data set. A slightly increased SSH OBE standard deviation helps to balance weights between different observation types (temperature/salinity and SSH) in the data assimilation system, and should be beneficial for analysis performance in general. An additional background check for SLA data after thinning should be considered in order to reject observations with large background departures. It is also worth to point out that SLA observations were not assimilated in ORAS5 outside the latitudinal band from 50°S to 50°N , nor in regions shallower than 500 m. This choice has been carried

over from ORAS4, and has been made for two reasons: i) to avoid assimilation of unreliable SLA data in the high latitudes and near the coast; ii) to take into account the fact that the NEMOVAR multivariate constraint for SLA-T-S is only valid in regions of strong vertical stratification. The first reason may no longer be valid, and it should be evaluated again following the recent development of the new ESA CCI sea-level product [Quartly et al., 2017, Legeais et al., 2018] which has reduced uncertainties in the high latitudes. An assessment of ORAS5 sea level with respect to this new sea-level observational product has been carried out in Section 3.3.2. The second reason is still relevant, but developments of multivariate constraints between the SLA and the barotropic stream function in NEMOVAR should result in much better use of altimeter data in mid and high latitudes.

2.5 Ensemble generation

A new generic ensemble generation scheme developed by perturbing both observations and surface forcings has been implemented in ORAS5. Here, we give a brief summary of the scheme, and we include a preliminary assessments of ORAS5 temperature and salinity ensemble spread. The reader should refer to Zuo et al. [2017a] for details about this ensemble generation scheme, including variable definitions quoted in the following discussions.

As a attempt to account for observation representativeness error, ORAS4 [Balmaseda et al., 2013] used superobbing and thinning methods to average or select observations toward scales resolved by the model. These methods have been enhanced in ORAS5 by adding a stratified random sampling method that can be applied to both surface and sub-surface observations. As a result of the random sampling, the different members of the ensemble see different observations. This is a way to optimize the number of the observations, since more observations are used in the ensemble. The in-situ observation profiles are perturbed in ORAS5 in two ways: by perturbing the longitude/latitude locations, and vertical perturbation by applying vertical stratified random thinning. The latitude/longitude locations of ocean in-situ profiles are perturbed so that the resulting locations are uniformly distributed within a circle of radius 50 km around the original location. This radius is chosen primarily considering observation representativeness error with respect to model horizontal resolution. The vertical thinning is applied to all in-situ observation profiles through stratified random sampling method that assumes a uniform distribution of locations within a given vertical range. A vertical thinning factor of 2 is used in ORAS5. This means that 2 observations within each model level, if available, are selected after thinning for data assimilation.

Perturbations to surface observations (SIC and SLA) in ORAS5 are applied primarily through a random thinning method. In all cases some pre-defined reduced grids are constructed in order to carry out thinning using stratified random sampling method, where observations within a given stencil in the reduced grid are randomly selected. As a result, each ensemble member assimilates slightly different observations. For SIC observation, this reduced grid is constructed with a length scale (L_{sic}) of approximately 30 km in the Arctic region. For SLA observation, this reduced grid is constructed with a length scale (L_{sla}) of approximately 100 km in the Tropics. These values were chosen to ensure a reasonable sample size within the reduced grid. Altimeter observations from different satellite missions are treated separately. This method ensures that the number of observation assimilated in each of the perturbed ORAS5 members is comparable to that in the unperturbed member.

A new method has been developed to perturb surface forcing fields used to drive ORAS5. This method preserves the multivariate relationship between different surface flux components, and has been used to perturb SST, SIC, wind stress, net precipitation and solar radiation. ORAS5 forcing perturbation takes into account both structural errors (SE), which are derived from differences between separate analyses data sets (e.g. wind stress differences between NCEP and ERA-40); and analysis errors (AE), which

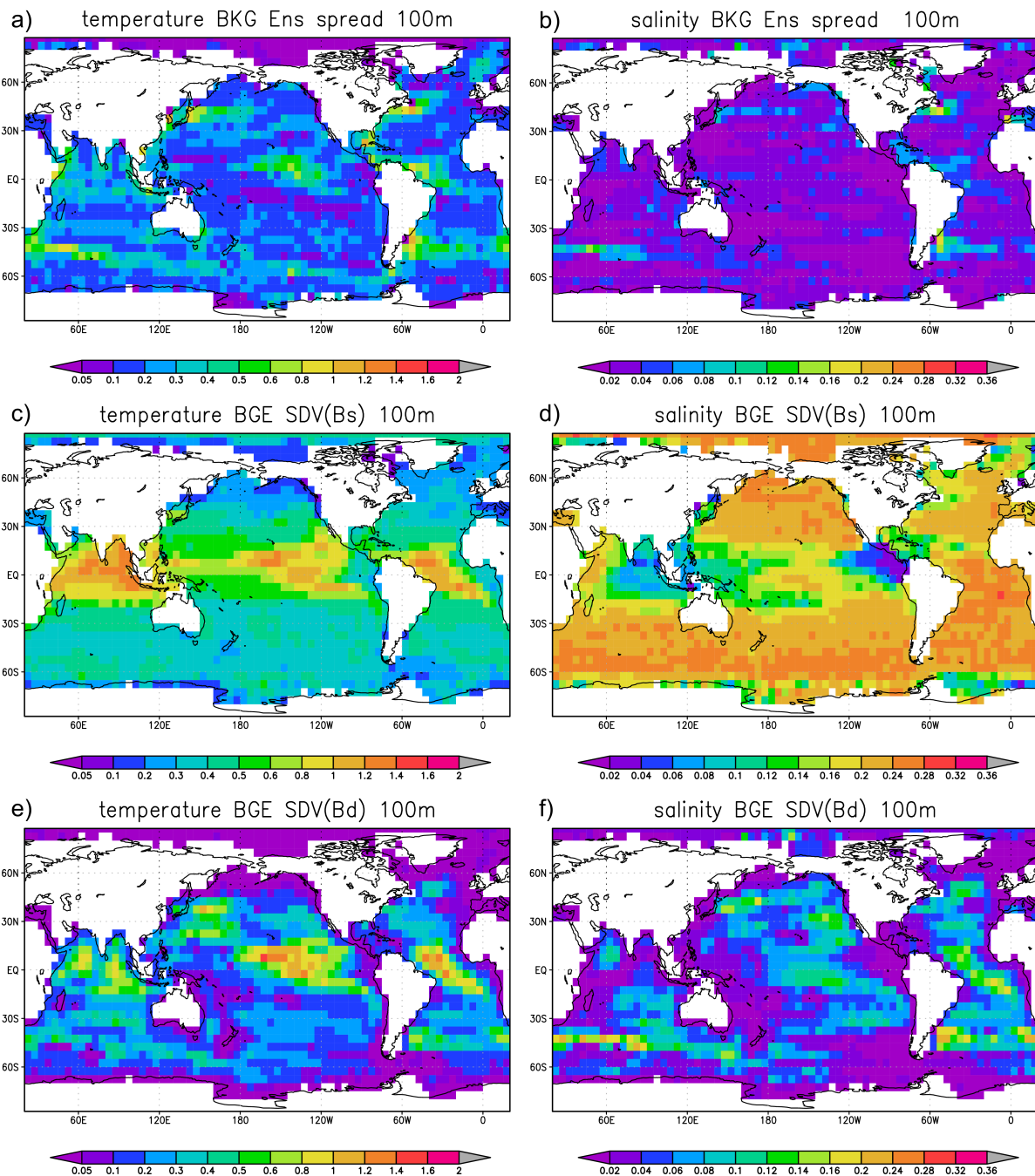


Figure 13: Maps of ORAS5 (a,b) ensemble spread, (c,d) specified BGE standard deviations and (e,f) diagnosed BGE standard deviations; (left) temperature in K and (right) salinity in psu. Ensemble spread is calculated using model background values from all ORAS5 ensemble members, averaged over the 2010–2013 period, and binned and averaged into $5^\circ \times 5^\circ$ lon/lat boxes.

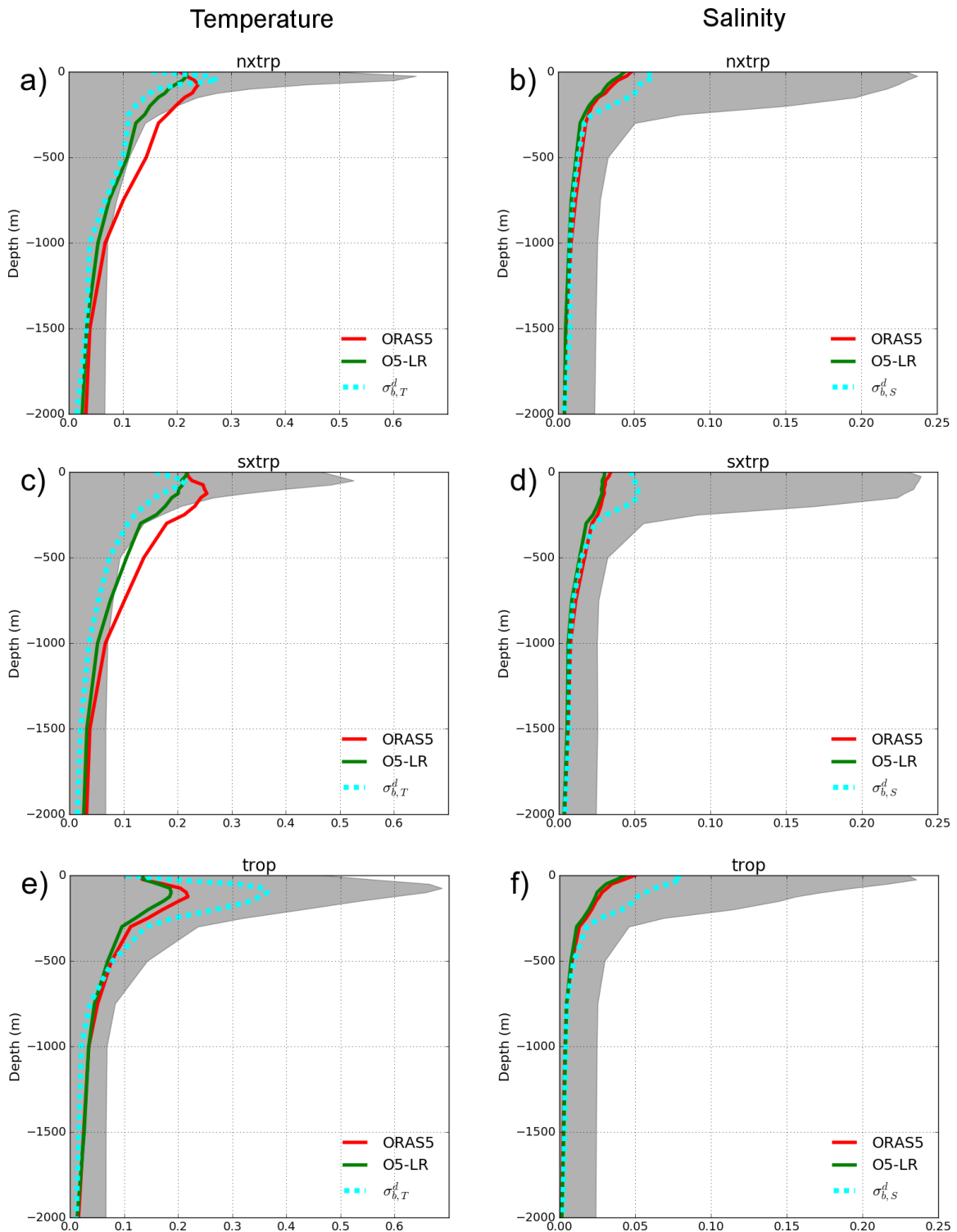


Figure 14: Vertical profiles of ensemble spread from ORAS5 (red solid lines) and O5-LR (see Table 4, green solid lines) for (left) temperature in K and (right) salinity in psu. Ensemble spread is calculated using model background values, temporally averaged over the 2010–2013 period, and spatially averaged over different ocean domains: (a,b) northern extra-tropics (nxtrp: 30°N to 70°N), (c,d) southern extra-tropics (sxtrp: 70°S to 30°S) and (e,f) tropics (trop: 30°S to 30°N). σ_b^d is the diagnosed BGE standard deviation from ORAS5 (cyan dashed lines) using Desroziers method; The specified BGE stand deviation is shown as the grey shaded area for reference.

are derived from differences between ensemble members within the same ensemble analysis (e.g. the 10 ensemble members of ERA20C [Poli et al., 2016]). The forcing in the ORAS5 control member remains unperturbed.

Following the same procedure described in Section 3.2 of [Zuo et al., 2017a], we compute the ORAS5 ensemble spread in observation space for the two primary ocean variables temperature and salinity. For verification purposes, both the specified model background error standard deviation (BGE STD) and the BGE STD diagnosed with the Desroziers method were computed for inter-comparison. Fig. 13 shows spatial maps of these variables at 100 m depth, after binning and averaging in $5^\circ \times 5^\circ$ lon/lat boxes. Here, temperature ensemble spread (Fig. 13a) shows a spatial pattern that is very similar to the diagnosed values using the Desroziers method (Fig. 13e), but with an amplitude that is reduced by approximately a factor of 2 in the Tropics. The salinity ensemble spread in ORAS5 (Fig. 13b) is in general under-dispersive when verified against diagnosed values (Fig. 13f), however the spatial patterns are similar. The specified BGE STD in ORAS5 is clearly overestimated for both temperature and salinity in the extra-tropics (Fig. 13c,d).

Fig. 14 shows averaged vertical profiles of diagnosed and specified BGE STD for the upper 2000 m. It is clear that ensemble spread of salinity is under-estimated almost everywhere in the upper 300 m in ORAS5 (Fig. 14b,d,f). In order to assess impact of model resolution, we include here results from O5-LR as well. The ensemble spread in O5-LR (green lines) is almost always smaller than that of ORAS5. However, there are with noticeable variations in that difference depending on region and depth range.

Despite the fact that ORAS5 does not include stochastic model perturbations and has a small ensemble of only 5 members, its ensemble spread is still considered to be a better estimation of BGE than the specified values used in the ocean analysis system. This indicates that specified model BGE STD can be improved by including this ensemble information in order to achieve better statistical consistency. This would also introduce a flow-dependent component into the NEMOVAR BGE covariances matrix by combining the ensemble-based and climatological estimation of BGE covariances.

2.6 The OCEAN5 Real-time analysis system

Based on ORAS5, a real-time ocean analysis system has been developed that forms the OCEAN5-RT component. This development has been done following a similar strategy as OCEAN4-RT (See Mogensen et al. [2012]). Unlike the historical ocean reanalysis, which is driven by atmospheric reanalysis forcing (e.g. ERA-interim) and assimilates re-processed observation data sets whenever possible; the OCEAN5-RT component relies on ECMWF NWP forcings and NRT observation data input (e.g. ocean in-situ observations directly from GTS and NRT altimeter data).

The OCEAN5-RT system became operational in November 2016, and started to provide the ocean and sea-ice initial conditions for the medium-range and monthly ensemble forecast (ENS) with the implementation of IFS Cycle 43r1 [Buizza et al., 2016]. Since November 2017, OCEAN5-RT also began to provide initial conditions for the new ECMWF long-range forecasting system SEAS5 [Stockdale et al., 2017]. In the most recent system upgrade with Cycle 45r1 in June 2018, the high-resolution deterministic forecast (HRES) has become coupled to the ocean and sea-ice model as well [Buizza et al., 2018], and started to take initial conditions from the OCEAN5-RT analysis. The atmospheric analysis system also replaced OSTIA SIC data, an external product that has been used since 2008, with the OCEAN5 SIC to constrain its lower boundary conditions (see Browne et al. [2018] for more details). As a result, the ocean data assimilation and analysis system are now more important at ECMWF than ever before. They are major components needed to deliver on ECMWF's Earth system strategy, with an ever stronger

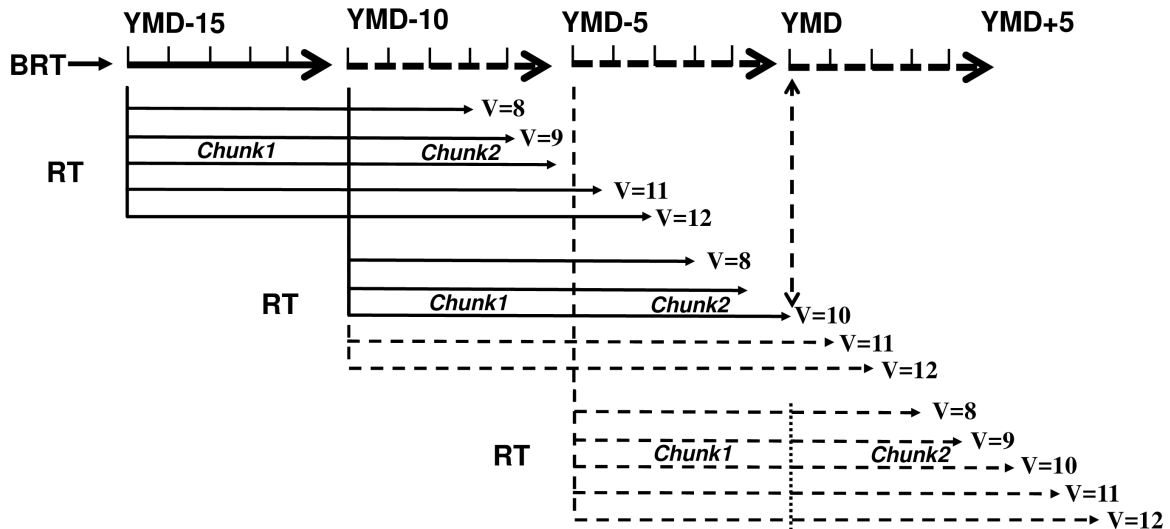


Figure 15: Schematic plot of OCEAN5 BRT and RT components: YMD=Current model date, V=Variable assimilation window length in the RT component. Solid lines denote analyses already produced in either BRT or RT component; dashed lines denote analyses not yet produced.

coupling between the atmosphere, land, waves, ocean and sea-ice components.

Fig. 15 shows schematically how the OCEAN5 suite, with its BRT and RT components, is implemented at ECMWF. The OCEAN5-BRT uses a 5-day assimilation window and is updated every 5 days with a delay D of 7 to 11 days. A minimum delay period of 7 days has been chosen in order to avoid a large degradation of the sea level analysis caused by delays in receiving NRT altimeter observations from the Copernicus Marine Environment Monitoring Service (CMEMS).

The OCEAN5-RT analysis is updated daily using a variable assimilation window of 8 to 12 days (equal to $D + 1$): starting from the last BRT analysis, it brings the RT analysis forward up to current conditions, to produced ocean states suitable to initialise the coupled forecast. This RT extension contains 2 assimilation cycles (Chunk) with a variable second assimilation window. The RT extension is always initialized from the last day of the BRT analysis and synchronically switches to the new initialization whenever the BRT analysis updates, hence the variable assimilation window. Taking current model day as YMD, then in Fig. 15 the RT assimilation window length for YMD is 10 days, and is initialized from YMD-10 BRT analysis. In practice, the OCEAN5 RT analysis is launched every day at 14Z (same as ORTS4) to produce a daily analysis valid for 00Z for the following day (YMD+1).

The surface forcing fields that drive the OCEAN5-RT component come from either ECMWF operational atmospheric analysis (AN), or ECMWF operational long forecast (FC), and include

- Solar radiation, net heat flux, and precipitation/evaporation, including snow (daily accumulation fields at 00Z everyday, from long forecast)
- Meridional/Zonal components of 10m wind speeds (instantaneous fields at 00/06/12/18Z everyday, from AN until YMD-1, then FC for YMD)
- 10m temperature and humidity (instantaneous fields at 00/06/12/18Z everyday, from AN until YMD-1, then FC for YMD)

- Wave effects from ECWAM: drag coefficient, north/east components of Stokes drift, normalized energy flux/wave stress into the ocean, 10m neutral wind speed, significant wave height and mean wave period (instantaneous fields at 00/06/12/18Z everyday, from AN until YMD-1, then FC for YMD)

All available observations are assimilated in the OCEAN5-RT analysis: in-situ temperature and salinity data from GTS network, sea level data from NRT satellite altimeter measurement, and daily-mean SIC and SST data from the OSTIA operational analysis. However, these may be different from the BRT. In the case of in-situ T/S and satellite, not all observations will be available at the start time or during the run time of the RT stream. There are also differences in the SST/SIC; since SST/SIC data for YMD is not available by the time the RT analysis is produced, they are persisted from the previous day (YMD-1). The 5 ensemble members of OCEAN5-RT daily analyses are then used to initialize the ocean and sea-ice components of all ENS members in a round robin method for the next day (YMD+1).

Fig. 16(top panels) show SST biases in OCEAN5-RT and OCEAN4-RT analyses against the OSTIA SST, for a randomly selected date as an example. In general, OCEAN5 RT has reduced SST bias almost everywhere compared to OCEAN4-RT, especially in the northern Pacific and at regions with strong eddy kinetic energy. This can be attributed primarily to the increased model resolution in OCEAN5, which allows more appropriate representation of eddies in the ocean. These are also regions where OCEAN5-RT ensemble has pronounced ensemble spread in SST (Fig. 16(bottom panels)). The SST ensemble spread from OCEAN5-BRT analysis is very similar to that of OCEAN5-RT. In addition, OSTIA SST analysis also shows large uncertainty in these regions (not shown). In ORTS4, relatively large SST ensemble spread (up to ~1 K) only exist at the eastern equatorial Pacific and Atlantic oceans.

The data infilling procedure involved in the conversion from Level-3 to Level-4 sea-ice analysis can lead to errors, e.g. the missing and/or corrupted swath data in L3 could be interpreted as zero SIC by the infilling method. To illustrate this problem, the OSTIA SIC for 3 consecutive days in April 2016 is shown in Fig. 17(top). The removal of SIC east of Greenland on 5th April and the spurious SIC in the Barents and Nordic seas on 7 April are the result from this OSTIA infilling procedure. This caused erroneous ocean initial conditions as well as forecasts. The forecast impact of 2m temperature was notable not just over the local region but also over wider Europe both in the medium and extended range (figure not shown). Nevertheless, the OCEAN5-RT component can provide us with a more robust SIC analysis (Fig. 17(bottom)). This is attributed to the dynamic-thermodynamic sea-ice model, a reasonable ocean thermal structure and surface forcing fields beneath and above the sea-ice respectively, as well as additional constraints from assimilating sub-surface in-situ observations in the OCEAN5-RT analysis. These additional constraints alleviate the problems found in the Level-4 observational SIC product. The coupling in HRES to OCEAN5-RT SIC also shows generally improved sea ice predictions in IFS Cycle 45r1 [Keeley and Mogensen, 2018]. However, it is worth to point out that the OCEAN5-RT SIC analysis is sensitive to weight assigned to input observation SIC. The impact of persisting OSTIA SIC in OCEAN5-RT for the last day is also visible in Fig. 17(bottom).

3 Assessment of ORAS5

3.1 Sensitivity experiments

Additional experiments have been conducted within the ORAS5 framework to help with assessment of different system components. These include sensitivities to different model resolutions, SST nudging

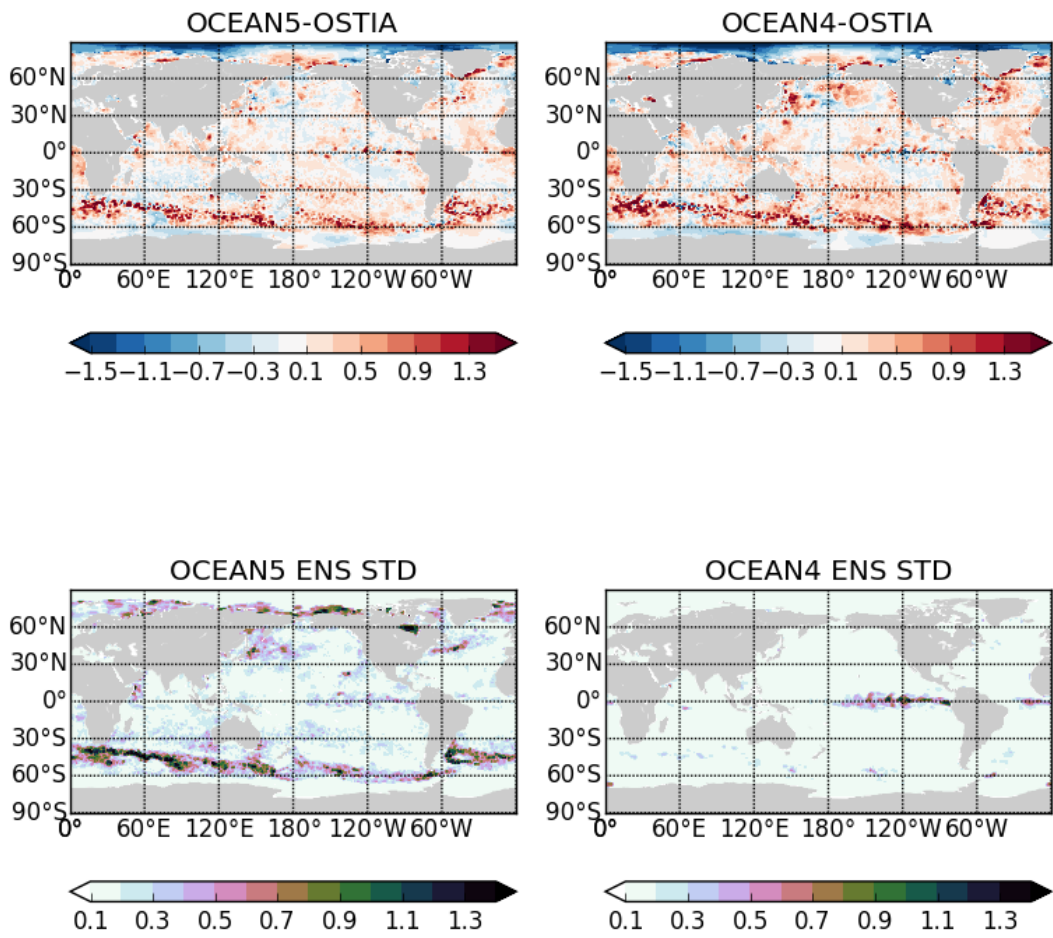


Figure 16: Daily-mean (top) SST biases and (bottom) SST ensemble spread from (left) OCEAN5-RT and (right) ORTS4, verified against OSTIA daily analysis on 15 August 2016. All units are K.

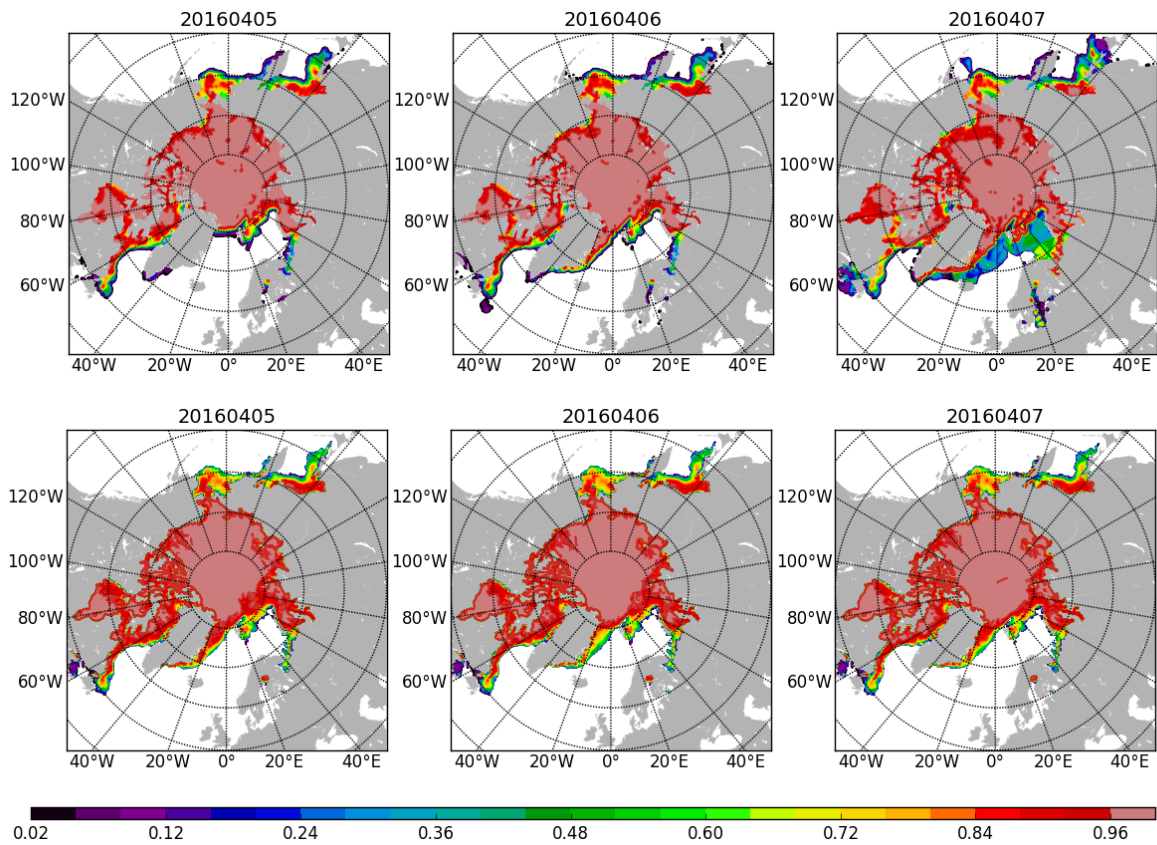


Figure 17: Arctic daily-mean SIC from (top) OSTIA analysis and (bottom) OCEAN5-RT analysis, from three consecutive days in April 2016 shown in columns 1 to 3.

strengths, assimilation of satellite altimeter data and bias corrections. Studies of other system parameters, e.g. OBE STD specification, have been carried out but are not discussed here for the sake of conciseness. A summary of system configurations of these sensitivity experiments can be found in Table 4. All sensitivity experiments cover the period 1979 to 2015, and are driven by the same surface forcing fields from ERA-interim. For all experiments except CTL-NoSST, SST are nudged to the HadISST2 product before 2008, and OSTIA operational analysis after 2008 (see Fig. 3). Unless noted otherwise, ORAS5 always refers to the control member of the reanalysis in all of the following discussions.

Table 4: Summary of ORAS5 sensitivity experiments

Name	Resolutions	SST nudging	Assim. SLA	Bias correction	notes
ORAS5	ORCA025.L75	YES	YES	YES	reference
CTL-NoSST	ORCA025.L75	NO	NO	NO	control run without DA
CTL-HadIS	ORCA025.L75	YES	NO	NO	control run with SST nudging only
O5-NoAlt	ORCA025.L75	YES	NO	YES	ORAS5 without SLA DA
O5-NoBias	ORCA025.L75	YES	YES	NO	ORAS5 without bias correction
O5-LR	ORCA1.L42	YES	ON	ON	ORAS5-equivalent in ORCA1.L42 resolution

3.2 Verification in observation space

Assessment of ORAS5 performance in observation space is carried out using model background errors with respect to all assimilated observations. We compute the model RMSE based on discrepancy between model background and observation for ORAS5 and all sensitivity experiments in Table 4. This approach allows to assess contributions from different system components and the performance of ORAS5 as an integrated reanalysis system. The reader should note that error statistics in CTL-NoSST and CTL-HadIS were computed in a observation space slightly differently (without vertical thinning of in-situ profiles) from other assimilation runs (ORAS5, O5-NoAlt, O5-NoBias). Assuming that there is no significant change in model error characteristics within some small vertical depth range (e.g. within 100 m), then this comparison between control runs and assimilation runs is still valid.

Time series of global mean RMSE in temperature and salinity from different sensitivity experiments are shown in Fig. 18. The cumulative number of assimilated observations of various types are also shown using the right y-axis. Mean vertical profiles of model RMSE for temperature and salinity can be found in Figures 19 and 20, respectively. Vertical profiles are temporally averaged from 2005 to 2014, when a

homogeneous global ocean observing network with Argo floats was available.

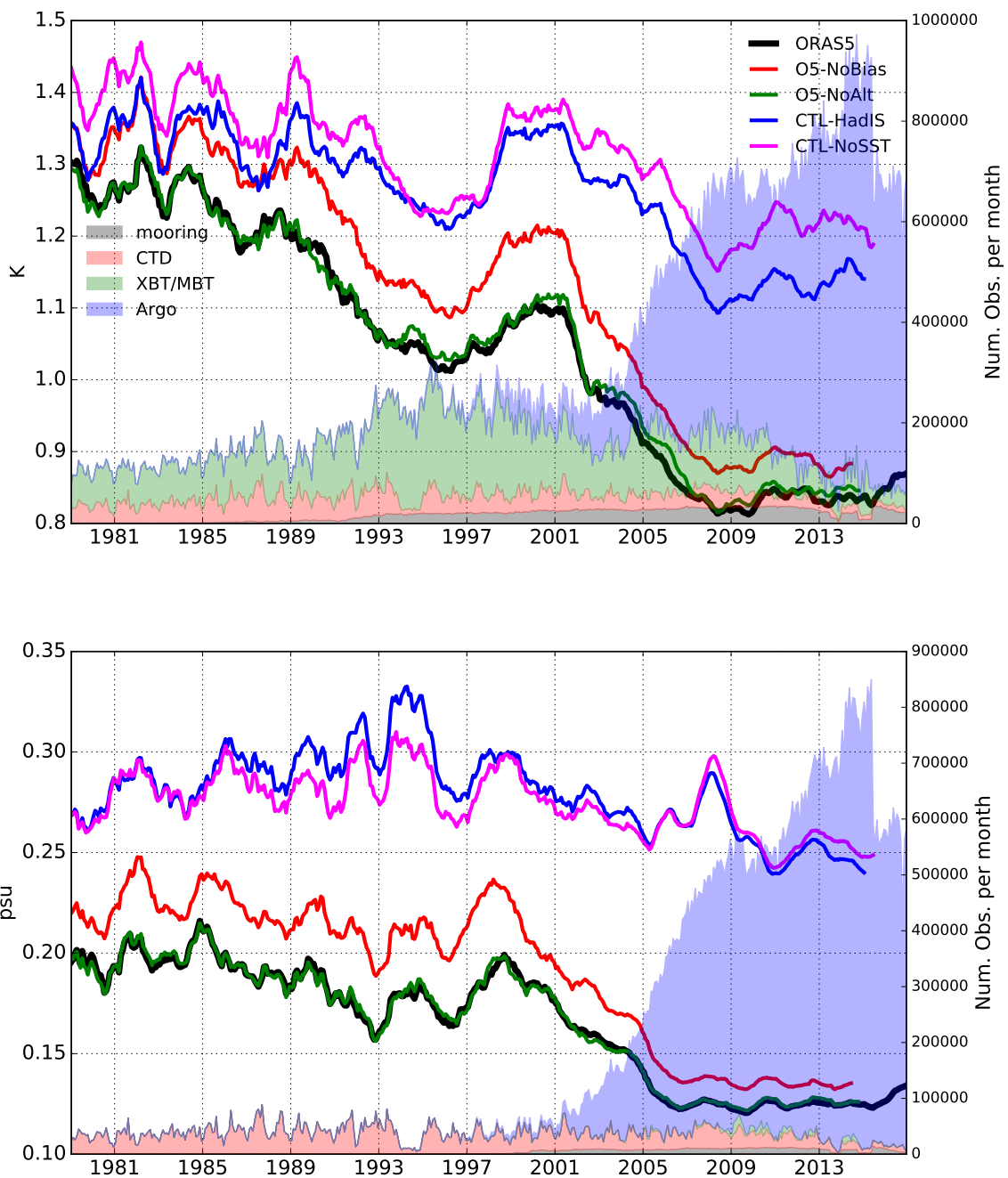


Figure 18: Time-series of model fit-to-observation RMSE in (top) temperature (K) and (bottom) salinity (psu) averaged over the upper 1000 m. Diagnostics are computed using model background departures from EN4 in-situ observations before June 2015, and departures from GTS observations from June 2015 on. RMSE are averaged over the global ocean, and a 12-month running mean is applied. Coloured patches and right y-axes show the cumulative number of observations from different sources assimilated per month in ORAS5.

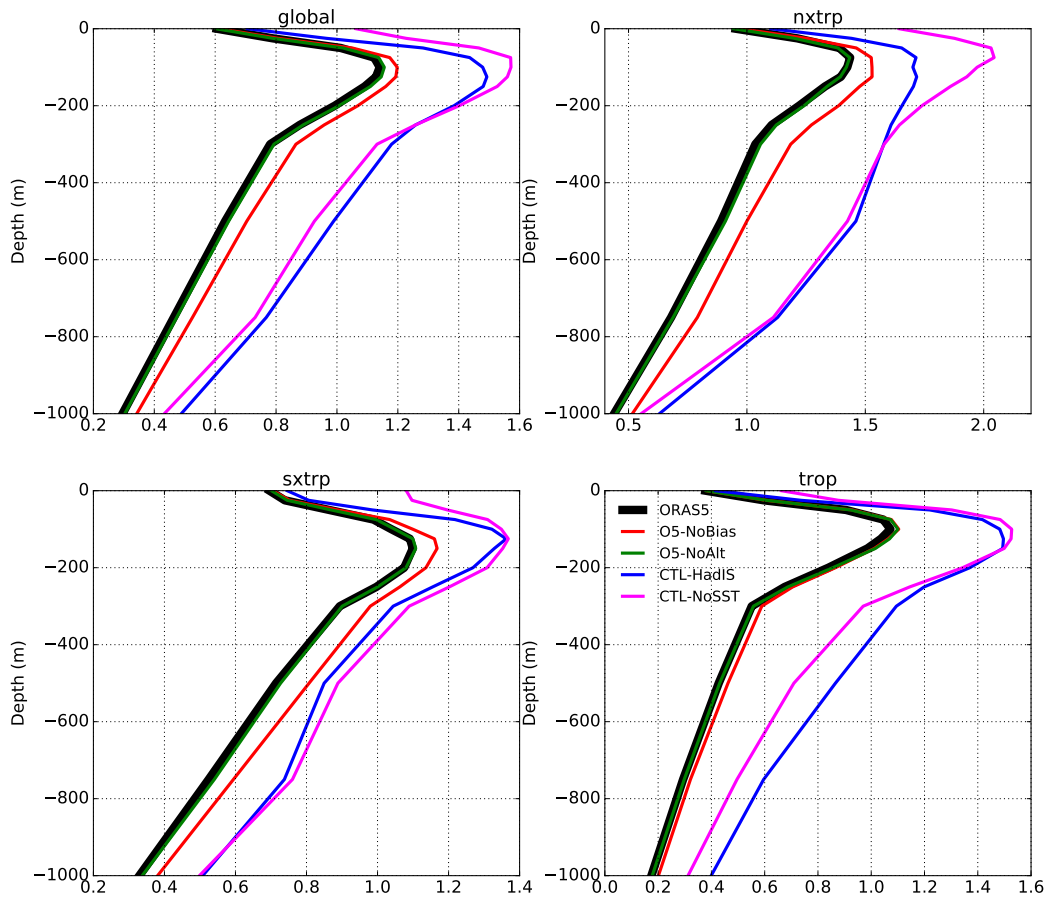


Figure 19: Vertical profiles of model temperature RMSE in K derived from different sensitivity experiments, averaged over the 2005–2014 period and over different ocean domains: (top-left) global, (top-right) northern extra-tropics 30°N to 70°N, (bottom-left) southern extra-tropics 30°S to 70°S, (bottom-right) Tropics 30°S to 30°N.

Overall, all components of the ocean reanalysis system (SST nudging, bias correction, assimilation of in-situ observation and altimeter data) contribute to reducing the model error, both in temperature (Fig. 18(top)) and salinity (Fig. 18(bottom)). However, by construction, some components have a more profound impact on the improvement of the ocean state, e.g. the assimilation of in-situ observations. The magnitude of RMSE reduction due to direct T/S assimilation can be derived from departure between O5-NoBias (red lines) and CTL-HadIS (blue lines), considering that altimeter data assimilation has almost no visible impact on the sub-surface ocean state (Fig. 19). The error reduction due to assimilation of in-situ data varies over time and is loosely proportional to the total number of observations assimilated. Over the Argo period 2005–2014, assimilation of in-situ data accounts for 65% of total RMSE reduction in temperature, and for nearly 90% of total RMSE reduction in salinity. These values are normalized against the total RMSE reductions which are derived from departures between ORAS5 (black lines) and CTL-NoSST (magenta lines). Note that CTL-NoSST also shows a declining trend in its fit-to-observation errors, especially following the introduction of the Argo floats (Fig. 18(top)). It is important to point out

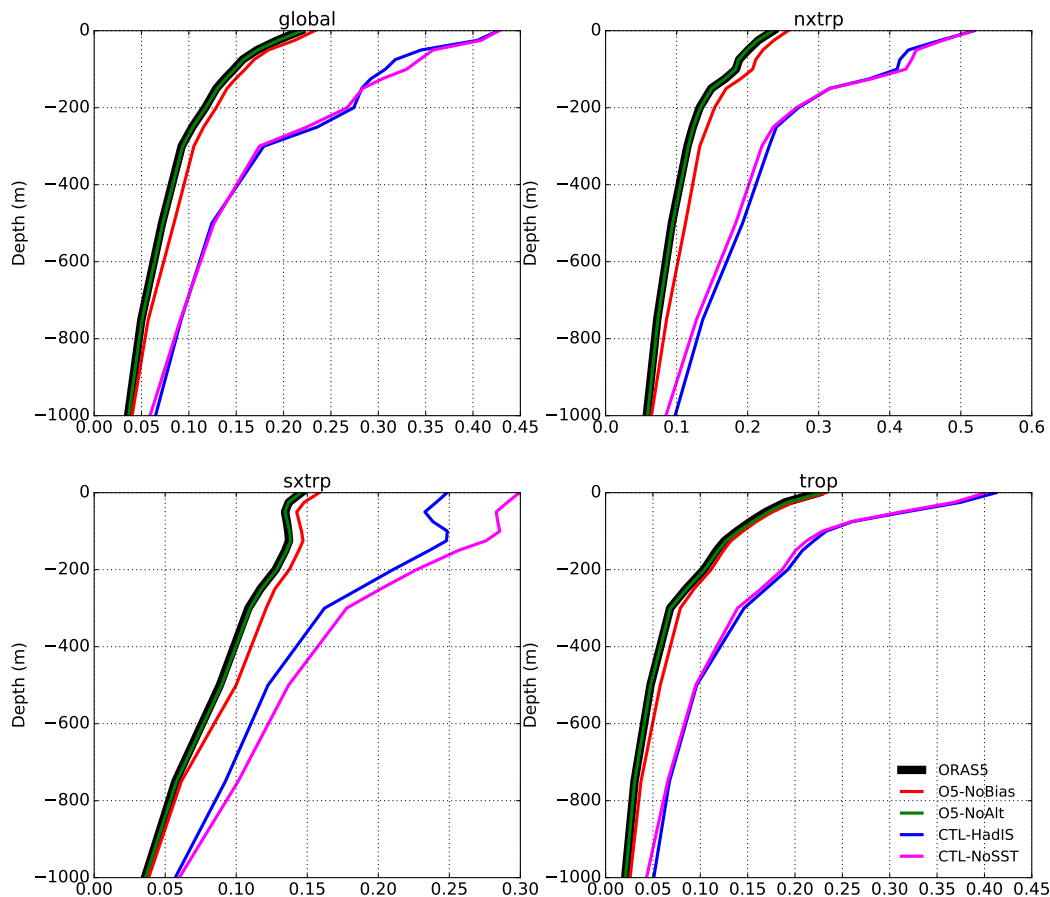


Figure 20: Same as Fig. 19 but for salinity (psu).

that this trend in CTL-NoSST does not represent a change of model errors over time, but is mainly a result of the evolving global ocean observing system. For instance, most southern extra-tropical ocean regions are only sampled with Argo floats. Therefore, global mean model fit-to-observation error reduces after including these extra regions, because (a) by construction, observation errors are larger near the coast than in the open ocean, and (b) there is much less land in the Southern than in the Northern Hemisphere. The readers should note that results in Fig. 18 are also subject to changes in the surface driving forcings, e.g. improvement in ERA-interim forcings due to better atmospheric observation coverage could result in reduced CTL-NoSST error as well.

The impact of the multi-scale bias correction scheme implemented in ORAS5 (see Section 2.3.3) can be derived from differences between O5-NoBias and ORAS5. This component plays an important role in correcting model errors, especially for the extra-tropical regions where the online bias term is applied as a direct correction to the T/S fields [Zuo et al., 2015]. Fig. 19 shows that the bias correction contributes to the total RMSE reduction with about 14% for temperature and about 10% for salinity, averaged for the upper 1000 m in the global ocean.

Differences between the CTL-NoSST and CTL-HadIS in global fit-to-obs RMSE give an estimate of surface SST nudging contributions. This component contributes about 18% to the global temperature error reduction (Fig. 18(top)). However, it leads to an increase of salinity errors between 1985 and 2005 (Fig. 18(bottom)). This deterioration can be as large as 10% in the mid 1990s.

SST nudging is globally the dominant term in temperature error reduction for the upper 200 m, but also leads to slightly increased temperature error in the Tropics below 300 m (Fig. 19). This degradation may be linked with the inappropriate partition of surface non-solar heat fluxes above and below the tropical thermocline, which is normally shallow than 200 m. During the Argo period, SST nudging also reduces the salinity RMSE at 100 m globally, as well as for the upper 1000 m in the southern extra-tropics (Fig. 20). For the upper 200 m of the southern extra-tropics, SST nudging accounts for nearly 40% (0.05 psu) of salinity RMSE reduction. This suggests that some unstable vertical density structures could persist in the model background for this region.

Other system components, like the assimilation of the altimeter data, lead to marginal improvements in global temperature (ca. 3% as derived from the difference between O5-NoAlt and ORAS5), and have mostly neutral impact on the model salinity errors. This result is very similar to ORAP5 [Zuo et al., 2017b], which indicates that the new SLA thinning scheme in ORAS5 is as effective as the superobbing scheme in representing observation representativeness error. Overall, we conclude that all system components in ORAS5 contribute to an improved ocean reanalysis when verified against in-situ observations.

3.3 Verification of ocean essential climate variables

Ocean essential climate variables (ECV) are ocean variables commonly used for monitoring ocean state and climate signals on decadal or longer time scales. SST, SLA and SIC are three main ocean ECV defined by the Global Climate Observing System (GCOS), and they have been selected here for an assessment of ORAS5 for climate applications. The ESA CCI project has developed suitable climate data records of these ECV, which are generally derived from a combination of satellite and in-situ observations. Here, the latest versions of these ESA CCI climate data records for SST, SLA and SIC were chosen to verify ORAS5 and some relevant sensitivity experiments. These observation-only analyses are considered independent from ORAS5, because they use different production systems and processing chains, and because they have not been assimilated in ORAS5. All statistics are computed using monthly-mean fields from ORAS5 and ESA CCI observation data sets interpolated to a common $1^\circ \times 1^\circ$ latitude–longitude grid.

3.3.1 Sea surface temperature

The ESA SST CCI (SST_cci) long-term analysis provides daily surface temperature of the global ocean over the period 1992 to 2010. Unlike the HadISST2 and OSTIA SST analyses, both of which are bias-corrected against in-situ observations (e.g. drifting buoys), ESA SST_cci only uses satellites observations (AVHRR and ATSR). Therefore, it provides an independent SST data set of a quality that is suitable for climate research. The latest version 1.1 of the ESA SST_cci [Merchant et al., 2016] data set (referred to as SST_cci1.1 hereafter), has been used here for verification of the performance of ORAS5 at the sea surface. The SST_cci1.1 data set is an update of version 1.0 described by Merchant et al. [2014].

Fig. 21 shows the bias, temporal correlation and RMSE of ORAS5 SST with respect to SST_cci1.1 between 1993 and 2010. For reference, ORAS4 (Fig. 21a,b,c) SST are also included here. Compared to ORAS4, ORAS5 (Fig. 21d,e,f) has reduced the warm SST bias in general, and has less SST bias in

the Gulf Stream extension, north of Iceland, and in the Southern Ocean. ORAS5 also shows increased temporal correlation with SST_cci1.1 in the Indian, South Pacific and Atlantic Oceans. In the equatorial Pacific, ORAS5 has visible maximum correlation values collocated with the Tropical Atmosphere Ocean (TAO) mooring arrays (Fig. 22). This suggests that the spatial correlation length-scale for these tropical moored buoys data is probably underestimated in ORAS5.

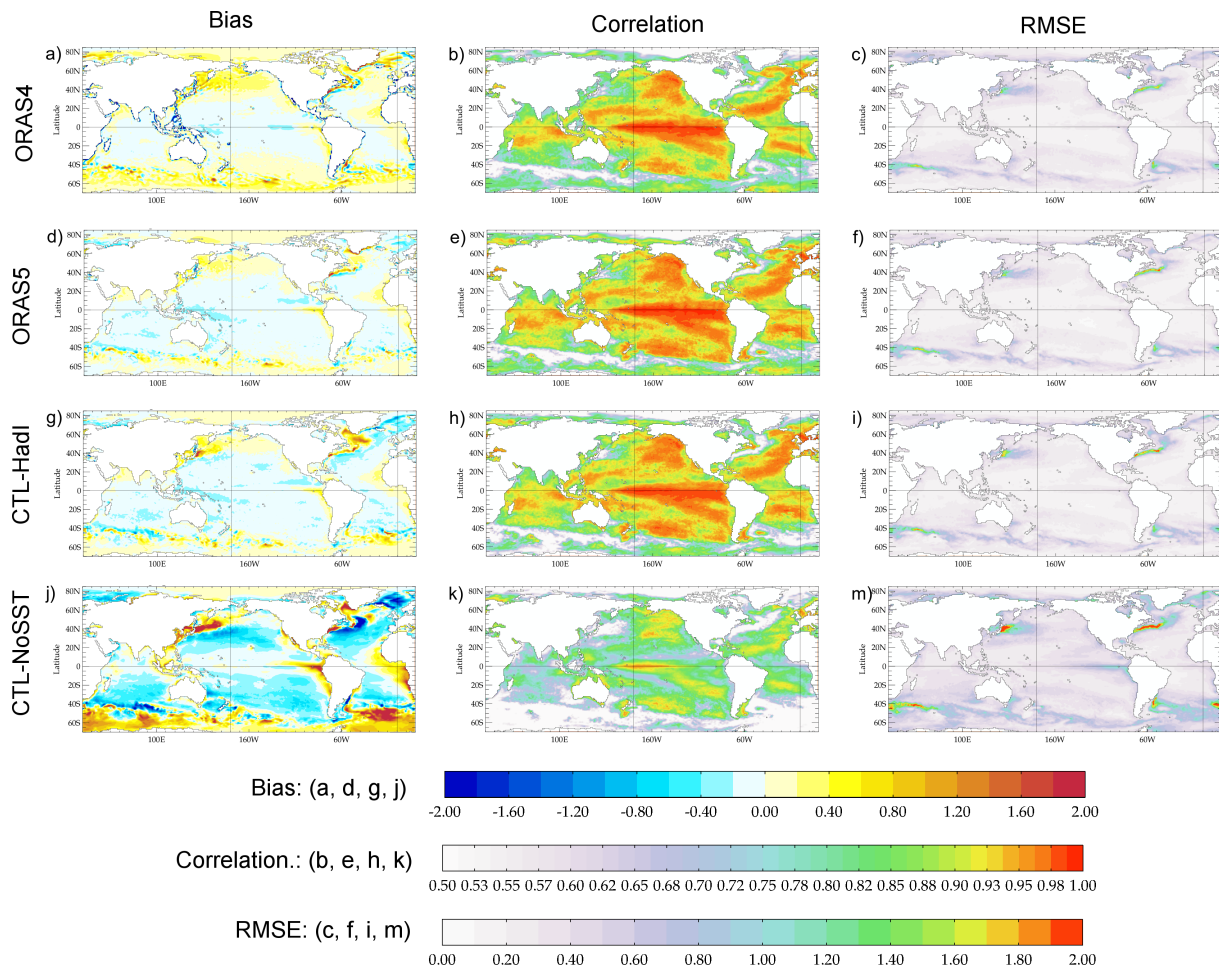


Figure 21: Characterisation of departures between modelled and observed SST: (left) bias in K, (middle) temporal correlations and (right) RMSE in K. Observed SST are from the SST_cci1.1 data set, and modelled SST are from (a,b,c) ORAS4, (d,e,f) ORAS5, (g,h,i) CTL-HadI and (j,k,m) CTL-NoSST. Statistics are computed using monthly-mean SST data 1993–2010, temporal correlation and RMSE are computed using monthly anomaly data after removal of the seasonal cycle. Note that correlations smaller than 0.5 are shown as white.

It is worth pointing out that different SST data sets were used for constraining the SST in ORAS4 and ORAS5: ORAS4 used OSTIA, and ORAS5 uses HadISST2. However, this cannot explain the differences between ORAS4 and ORAS5 seen in Fig. 21. To the contrary: w.r.t. SST_cci1.1, OSTIA has higher temporal correlation and reduced mean differences than HadISST2 in the extra-tropics (Fig. 23). This is presumably because the SST_cci1.1 and OSTIA were produced using the same optimal interpolation system. Improvements in ORAS5 can be attributed to increased model resolution and assimilation of updated in-situ observation data set (see Section 2.3).

Differences between ORAS5 (Fig. 21d,e,f) and CTL-HadIS (Fig. 21g,h,i) are non-trivial, with largely

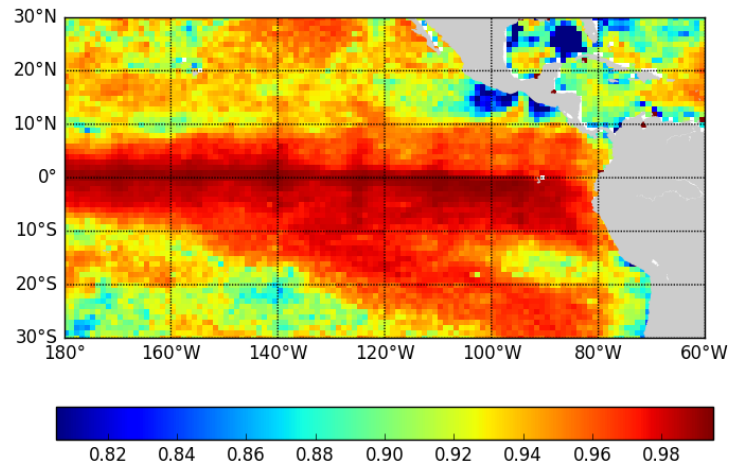


Figure 22: Temporal correlations between ORAS5 and observed SST from the SST_cci1.1 data set, as a zoom in the TAO mooring location in the tropical Pacific from Fig. 21e. Note that only correlations larger than 0.8 are shown here.

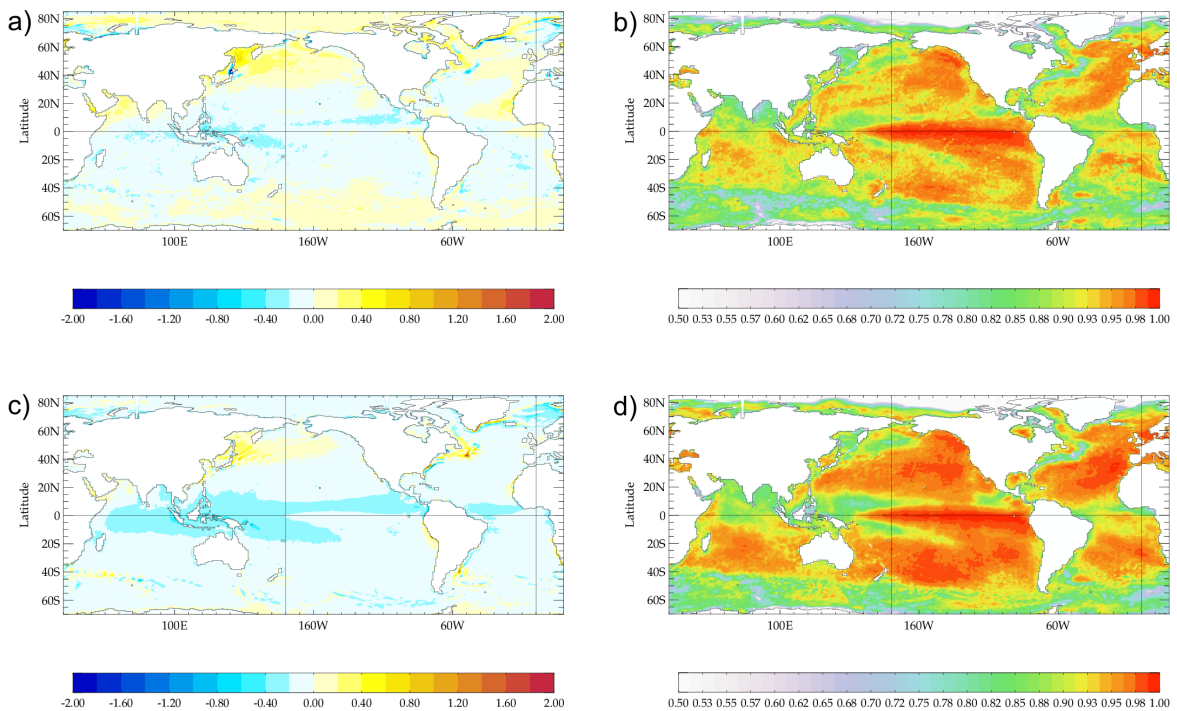


Figure 23: Characterisation of differences between the observational SST data sets HadISST2, OSTIA and SST_cci1.1: (left) mean difference in K and (right) temporal correlations of (a,b) HadISST2 and SST_cci1.1 and (c,d) OSTIA and SST_cci1.1. Statistics are computed in the same way as in Fig. 21.

reduced mean biases in ORAS5, especially for the Labrador Sea and East of Japan. These regions also have the least temporal correlation with SST_cci1.1 data due to misrepresentation of mixed layer depth in CTL-HadIS, but are slightly improved in ORAS5 by assimilating in-situ observations. As expected, CTL-NoSST has the largest SST biases with respect to SST_cci1.1. These biases are associated with systematic model and/or forcing errors, e.g. underestimated upwelling west of South America and South Africa, misrepresentation of mixing in the Southern Ocean, or others. The difference between CTL-NoSST and CTL-HadIS highlights the fact that the SST nudging method is very effective in keeping SST close to observations in the reanalysis system. However, ORAS5 SST is still performing poorly in areas with strong currents, especially for the Gulf Stream and its extensions. Therefore, work toward SST assimilation using the full 3DVAR-FGAT configuration should be encouraged in the future development.

3.3.2 Sea level

The ESA sea-level CCI (SL_cci) project provides long-term along-track and gridded sea-level products from satellites for climate applications. Here, we use the latest reprocessed version 2.0 data from SL_cci (hereafter called SL_cci2) for validation of modelled sea level. The SL_cci2 sea-level data is an update of version 1.1 [Ablain et al., 2015] and includes data from additional altimeter missions (SARAL/AltiKa and CryoSat-2). Unlike the AVISO DT2014 product, which is dedicated to the best possible retrieval of meso-scale signals, SL_cci2 data focuses on the homogeneity and stability of the sea-level record. It has been produced using a different processing chain, and it also uses new altimeter standards, including a new orbit solution, atmospheric corrections, wet troposphere corrections, and a new mean sea-surface and ocean-tide model (see Quartly et al. [2017]). Therefore, the SL_cci2 sea-level can be considered as an independent data set for the verification purpose.

The inter-annual variability of regional sea level can be evaluated using temporal correlation between model SLA and SL_cci2 gridded SLA data. Fig. 24(left panels) shows temporal correlation maps for the 2004–2013 period, including results from ORAS4 as a reference. In general, ORAS5 shows patterns of high correlation that are very similar to ORAS4, however correlation is improved almost everywhere except for the western tropical Pacific (Fig. 24c). This improvement can in large parts be attributed to the eddy-permitting model resolution of ORAS5, which accounts for most improvement in the subtropics, and the assimilation of the new AVISO DT2014 data set (see Section 2.4), which accounts for most improvement in the tropics.

The degradation in the western tropical Pacific is probably linked to sub-optimal parametrization in the ORAS5 data assimilation system. For instance, SLA observations in this area have been given much less weight in ORAS5 compared to ORAS4 because a large number of small islands are only resolved by ORAS5. This has already been found for ORAP5 [Zuo et al., 2017b].

The strong correlation near the Arctic sea-ice edge in ORAS5 suggests improved geostrophic circulation in the Arctic ocean, despite no SLA data being assimilated in this region. As expected, assimilation of altimeter SLA data significantly improves model performance, as demonstrated by the increased correlation in ORAS5 compared to O5-NoAlt (Fig. 24e). In addition, assimilation of ocean in-situ observations further improves representation of sea level in the reanalysis due to better representation of meso-scale dynamics. This is most pronounced in the extra-tropical regions, as demonstrated by differences between O5-NoAlt and CTL-HadIS (Fig. 24g).

For reference, the same diagnostics have been carried out for AVISO DT2014 data with respect to SL_cci2 (Fig. 25). In general, the temporal correlation between DT2014 and SL_cci2 is very high, indicating excellent agreement of temporal variations between the two data sets. Regions with lower

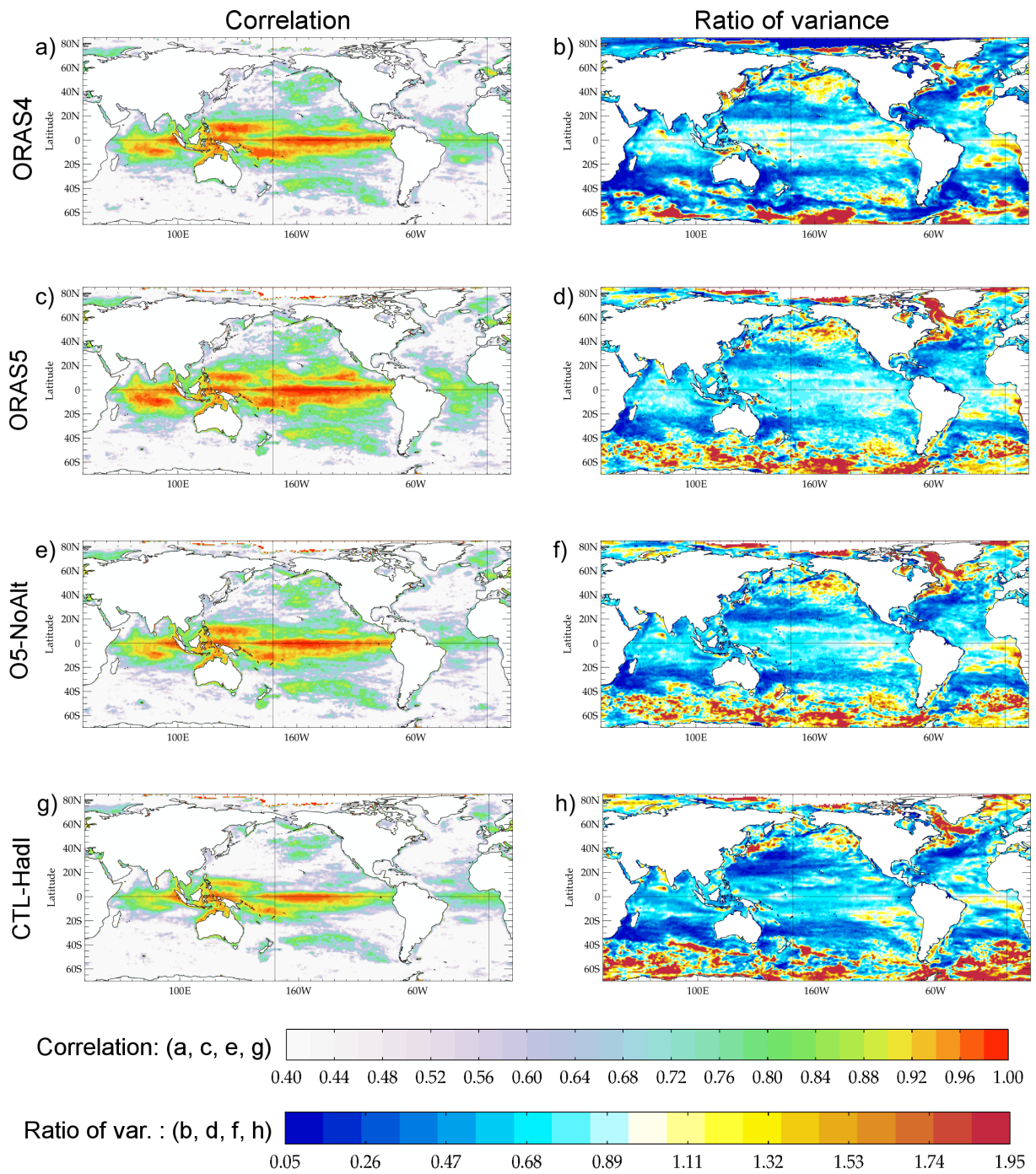


Figure 24: Characterisation of departures between modelled and observed SLA: (left) temporal correlations and (right) ratio of variance between SLA from model and SL_cci2. Model SLA are from (a,b) ORAS4, (c,d) ORAS5, (e,f) O5-NoAlt and (g,h) CTL-HadIS. Statistics are computed using monthly-mean SLA data over the 2004–2013 period, temporal correlation has been diagnosed after removal of the seasonal cycle. Note that correlations smaller than 0.4 are shown as white.

correlation are visible though, e.g. along the North Equatorial Countercurrent in the Pacific between 180°W and 100°W (Fig. 25a). This is likely associated with differences in the production chains between DT2014 and SL_cci2, which include different altimeter-mission-dependent orbit solutions and

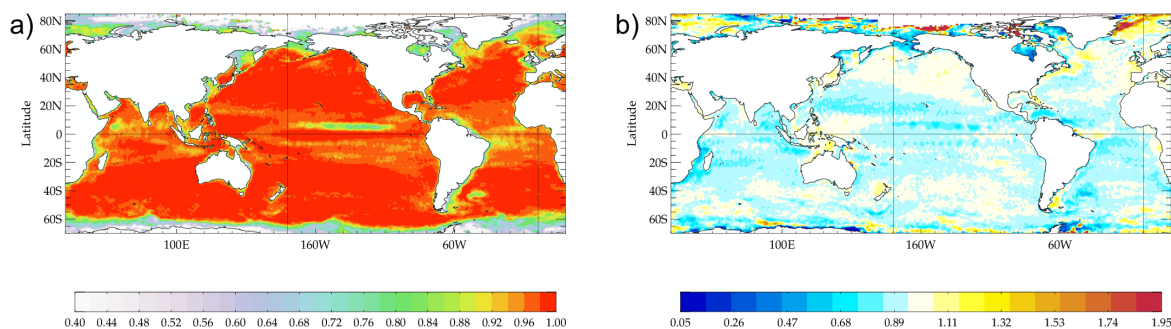


Figure 25: (a) SLA correlation and (b) ratio of variance between AVISO DT2014 and SL_cci2 data. Statistics are computed following the same way in Fig. 24.

geophysical corrections and different filtering methods in processing along-track SLA. This discrepancy between different observational data sets is also responsible for the low correlation between ORAS5 and SL_cci2 SLA in the same region.

In order to evaluate the magnitude of temporal SLA variance in ORAS5, we compute the ratio of SLA variance between model and SL_cci2 for the 2004–2013 period, with results shown in Fig. 24(right). Compared to SL_cci2 data, both ORAS4 (Fig. 24a) and ORAS5 (Fig. 24b) underestimate SLA variance. The global mean SLA variance in ORAS4 is about half of the SL_cci2 estimate, mostly because ORAS4 is incapable of resolving meso-scale activity and assimilates SLA through a superobbing scheme. This problem has been alleviated by increasing the model resolution and using a new SLA thinning scheme in ORAS5 (see Section. 2.4).

However, ORAS5 still underestimates SLA variance by approximately one third in the average grid cell. Some of this underestimation is attributed to the assimilated DT2014 data set, which has about 10% less variance than SL_cci2 in the average grid cell (see Fig. 25b). This difference between SL_cci2 and DT2014 is mostly due to different geophysical corrections used in production (Jean-Francois Legeais, personal communication). Removal of altimeter data (O5-NoAlt, Fig. 24c) and in-situ data (CTL-HadIS, Fig. 24d) from the assimilation system further reduces simulated SLA variances, by approximately 2% and 4%, respectively. There are regions where ORAS5 has larger SLA variance though, e.g. in the Baffin Bay, Hudson Bay, and most areas in the Southern Ocean. Additional evaluations of ORAS5 sea level with respect to AVISO DT2014 and other ESA Sea Level CCI products have been carried out in Section 5.2 of [Legeais et al. \[2018\]](#).

3.3.3 Sea-ice concentration

The ESA Sea-Ice CCI (SI_cci) project has produced a long-term SIC data set based on satellite passive microwave radiances. The latest version 1.1 SIC data from SI_cci (hereafter SI_cci1.1) was produced using a sea-ice concentration algorithm and methodology developed by EUMETSAT Ocean and Sea Ice Satellite Application Facility [[Sørensen and Lavergne, 2017](#)]. This SI_cci1.1 data set is available from 1993 to 2008 in 25 km resolution, and is used here for the evaluation of the ORAS5 sea ice.

Fig. 26 shows maps of model SIC RMSE based on departures between model SIC and SI_cci1.1 data, averaged over the 1993–2008 period. ORAP5 is a pilot reanalysis before ORAS5, and its ability to represent Arctic sea-ice has been documented to be reasonably good [[Tietsche et al., 2015](#), [Chevallier et al., 2017](#), [Uotila et al., 2018](#)]. Therefore, ORAP5 has been retained here as a reference. Spatial pattern

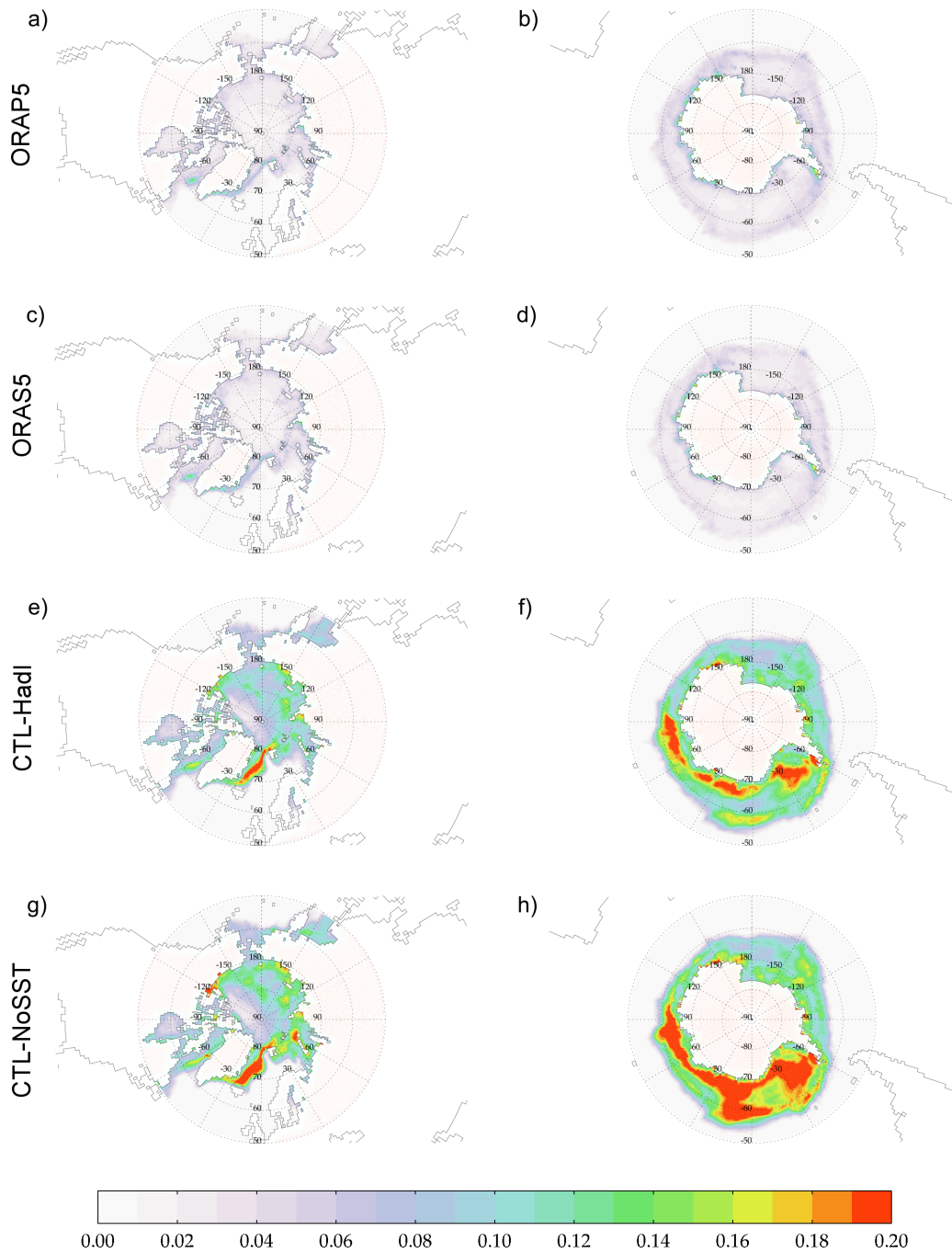


Figure 26: RMSE of model SIC departures with respect to SI_cci1.1 SIC data in (left) the Arctic and (right) the Antarctic; model SIC are from (a,b) ORAP5; (c,d) ORAS5, (e,f) CTL-HadIS and (g,h) CTL-NoSST. Statistics are computed using monthly anomaly SIC data over the 1993–2008 period, with seasonal signals removed.

and magnitude of ORAS5 SIC errors (Fig. 26c,d) are very similar to that of ORAP5 (Fig. 26a,b) in polar regions. In the Arctic, ORAS5 has the largest SIC RMSE in the Labrador Sea and east coast of Greenland during winter. This is attributed to model errors in the NEMO-LIM2 model as documented by [Tietsche et al. \[2015\]](#).

Assimilation of OSTIA SIC has greatly improved sea-ice performance in ORAS5. Compared to CTL-HadIS (Fig. 26e,f), ORAS5 has reduced SIC RMSE almost everywhere except for the Canadian Arctic where the thickest sea ice exists. The largest improvement is located at the east of Greenland along the south edge of the Arctic sea-ice outflow extension, which is likely due to model errors in ocean current and/or sea-ice velocity. The SST nudging scheme also contributes to reduction of SIC RMSE in the system. The differences in SIC RMSE between CTL-HadIS and CTL-NoSST (Fig. 26g,h) are mostly due to correction of thermodynamic errors in the model. Similar conclusions can be drawn for sea-ice conditions in the Antarctic as well. Both ORAS5 and ORAP5 show visible SIC RMSEs along the coast of Antarctic, which can be attributed to misrepresentation of polynya in the model and/or ERA-interim forcing error in these regions.

An evaluation of ORAS5 sea-ice thickness in the Arctic has been carried out by [Tietsche et al. \[2018\]](#) with a focus on thin sea ice with respect to a data set derived from L-band radiances from the SMOS satellite L-Band. An additional study of ORAS5 sea-ice conditions and the sea-ice extreme event in 2016 can be found in [Zuo et al. \[2018\]](#).

4 Summary

ORAS5 is a state-of-the-art 0.25° resolution ocean and sea-ice ensemble reanalysis that covers the period from 1979 to present. ORAS5 and its real-time extension constitute OCEAN5, the fifth generation of ECMWF's ocean reanalysis-analysis system. OCEAN5 became operational in November 2016. Major improvements of ORAS5 w.r.t. ORAS4 are the inclusion of a sea-ice reanalysis, increased resolution in the ocean, improved and up-to-date observational data sets, and improved methods for ensemble generation.

ORAS5 has been developed based on ORAP5, a pilot system, with a series of system updates. These include:

- updated data assimilation with the latest observational data sets (EN4 for in-situ temperature and salinity and DT2014 altimeter-derived sea level anomalies) together with improved observation quality-control methods,
- improved temporal consistency of the SST/SIC observation data,
- a new ensemble generation scheme that accounts for both observation representative error and multivariate errors in surface forcing,
- revised spin-up ensemble for the initialization of the reanalysis,
- revised offline bias correction estimation based on ensembles,
- revised bias correction scheme with stability check to prevent static instability,
- revised observation pre-processing,
- and a faster method to estimate the MDT needed for SLA assimilation.

These system updates are described in detail in this document, including an evaluation of system performance in the context of data assimilation.

The OCEAN5 RT analysis is produced daily, and is used to initialize the ocean and sea-ice components of all ECMWF forecasts (ENS, HRES and SEAS5). Initialized from the latest ORAS5 conditions, the RT extension is produced by assimilating all available observational data into the ocean model driven by atmospheric analysis and NWP forcing. Differences to ORAS5 are the variable assimilation window length, the smaller number of observations used, and the atmospheric forcing, SST and SIC data sets used during in the final day of the RT extension. The RT analysis is essential for the timely initialization of the ECMWF coupled forecasts, and it has enabled the recent use of the coupled model in the HRES forecast (Cy45r1 update).

The climate variability of ORAS5 has been evaluated using independent temporal records of SST, SLA and SIC. These three ECVs records have been produced by the ESA CCI project. In general, ORAS5 shows improved ocean variability compared to ORAS4, in both SST and SLA. The performance of SIC in ORAS5 is as good as ORAP5, which has been recognized by many as one of the best products for reconstructing historical sea-ice conditions. Evaluations of ORAS5 have also been carried out within the framework of ESA SL_cci [Legeais et al., 2018], SPICES [Tietsche et al., 2018] and CMEMS projects [Zuo et al., 2018].

The large SST biases in the Gulf Stream and its extensions have improved in ORAS5 compared to ORAS4, as a consequence of increased spatial resolution. However, the bias remains large, and is associated with a fundamental misrepresentation of front positions and overshoot of the northward transport along the coast after Cape Hatteras. The impact of high resolution in ORAS5 is more visible in the area of the sub-polar gyre. Preliminary results from a sensitivity study (not shown) suggest that some ocean circulation indices are sensitive to the strength of the SST nudging, which may be too strong in ORAS5. Other issues identified in ORAS5 that need improving include the usage of observations in high latitudes, near the coast and on the continental shelf, underestimated SLA variances associated with sub-optimal parameter specifications in observation errors and data sampling, abrupt Antarctic sea-ice changes in 1986 due to missing-data events in the OSTIA SIC product. It is recommended that assimilation of Level-3 SIC data from OSI-SAF instead of Level-4 OSTIA data should be exploited in the development of next system.

Two clear priorities for developments of the ocean data assimilation system emerge from the experience with ORAS5. One is the treatment of SST observational constraints. The other required improvement is related with the assimilation of altimeter-derived sea level. The current relaxation method to constrain the SST has several shortcomings: i) it lacks the capability to project directly the SST information into the subsurface, relying on the ocean model mixing processes to achieve that; ii) the strength of the relaxation at high latitudes can have strong impacts on the ocean circulation, introducing process imbalance which damage the coupled forecast. The latter is the subject of a more detailed study (in preparation). It would be possible to optimize the strength of the SST nudging; but a longer-term solution requires investing in the proper assimilation of SST, using an appropriate vertical and horizontal correlation structure function and multivariate relationships. The assimilation of altimeter-derived sea level should also be improved. The current practice of assimilating sea level anomalies (SLA) requires a pre-computed mean dynamic topography (MDT), which is expensive, or even unaffordable in coupled data assimilation, and it is prone to errors. Better solutions should be sought in terms of an online computation of the MDT [Lea et al., 2008], or, preferably, by making direct use of sea surface height and geoid information. The use of altimeter observations should also be optimized by further development of the multivariate background error covariance formulation in NEMOVAR, so as to include constraints between sea surface height and barotropic stream function. This should have a large impact in constraining the position of the Gulf Stream and other oceanic fronts, which should benefit the NWP forecasting activities.

Appendix

Readers who are interested in the sensitivity experiments discussed in this report can refer to Table 5 and 6 for the corresponding experiment IDs as they were archived in ECFS.

Table 5: Experiment IDs for ensemble pre-production runs

Name	Exp. ID	Name	Exp. ID
INI1	g5jr	BIAS1	g6vi
INI2	g61a	BIAS2	g8dn
INI3	g8sj	BIAS3	g8s4
INI4	g7f1	BIAS4	g8sc
INI5	g7f7	BIAS5	g8uv

Table 6: Experiment IDs used for testing ORAS5 configurations

Name	Exp. ID	Name	Exp. ID	Name	Exp. ID	Name	Exp. ID
ASM-HadI	g8tf	EXP3	gdwr	PC-OFF	g8nz	NoCap	g6z2
ASM-OST	g8s1	EXP4	gdwy	PC-ON	g9ky	CP10	g7f0
ASM-HadI-OST	g8tx						

Acknowledgements

Development of the ORAS5 ocean reanalysis system has been supported by ESA through the sea-level CCI project, by the Copernicus Marine environment monitoring service (CMEMS) through the GLO-RAN project, and by the EU H2020 programme through the AtlantOS project. The production of ORAS5 has been funded by the Copernicus Climate Change Service. ECMWF implements this Service and the Copernicus Atmosphere Monitoring Service on behalf of the European Commission.

References

- M. Ablain, A. Cazenave, G. Larnicol, M. A. Balmaseda, P. Cipollini, Y. Faugère, M. J. Fernandes, O. Henry, J. A. Johannessen, P. Knudsen, O. Andersen, J. Legeais, B. Meyssignac, N. Picot, M. Roca, S. Rudenko, M. G. Scharffenberg, D. Stammer, G. Timms, and J. Benveniste. Improved sea level record over the satellite altimetry era (1993–2010) from the Climate Change Initiative project. *Ocean Science*, 11(1):67–82, 1 2015. ISSN 1812-0792. doi: 10.5194/os-11-67-2015. URL <http://www.ocean-sci.net/11/67/2015/>.
- M. A. Balmaseda. Ocean analysis at ECMWF: From real-time ocean initial conditions to historical ocean reanalysis. *ECMWF Newsletter*, 105:24–42, 2005. URL <http://www.ecmwf.int/publications/newsletters/pdf/105.pdf>.
- M. A. Balmaseda, A. Vidard, and D. L. T. Anderson. The ECMWF Ocean Analysis System: ORA-S3. *Monthly Weather Review*, 136(8):3018–3034, 2008. ISSN 0027-0644. doi: 10.1175/2008MWR2433.1. URL <http://journals.ametsoc.org/doi/abs/10.1175/2008MWR2433.1>.
- M. A. Balmaseda, K. Mogensen, and A. T. Weaver. Evaluation of the ECMWF ocean reanalysis system ORAS4. *Quarterly Journal of the Royal Meteorological Society*, 139(674):1132–1161, 7 2013. ISSN 00359009. doi: 10.1002/qj.2063. URL <http://doi.wiley.com/10.1002/qj.2063>.
- B. Bernard, G. Madec, T. Penduff, J.-M. Molines, A.-M. Treguier, J. Le Sommer, A. Beckmann, A. Biastoch, C. Böning, J. Dengg, C. Derval, E. Durand, S. Gulev, E. Remy, C. Talandier, S. Theetten, M. Maltrud, J. McClean, and B. De Cuevas. Impact of partial steps and momentum advection schemes in a global ocean circulation model at eddy-permitting resolution. *Ocean Dynamics*, 56(5-6):543–567, 12 2006. ISSN 1616-7341. doi: 10.1007/s10236-006-0082-1. URL <http://link.springer.com/10.1007/s10236-006-0082-1>.
- S. C. Bloom, L. L. Takacs, A. M. Da Silva, and D. Ledvina. Data assimilation using incremental analysis updates. *Monthly Weather Review*, 124(6):1256–1271, 1996.
- Ø. Brevik, K. Mogensen, J.-R. Bidlot, M. A. Balmaseda, and P. A. Janssen. Surface wave effects in the NEMO ocean model: Forced and coupled experiments. *Journal of Geophysical Research: Oceans*, 120(4):2973–2992, 2015. ISSN 21699291. doi: 10.1002/2014JC010565.
- P. Browne, P. d. Rosnay, H. Zuo, A. Bennett, and A. Dawson. Weakly coupled oceanatmosphere data assimilation in the ECMWF NWP system. *ECMWF Technical Memorandum*, 2018.
- R. Buizza, J. R. Bidlot, M. Janousek, S. Keeley, K. Mogensen, and D. Richardson. New IFS cycle brings sea-ice coupling and higher ocean resolution. *ECMWF Newsletter*, 150:14–17, 2016.
- R. Buizza, G. Balsamo, and T. Haiden. IFS upgrade brings more seamless coupled forecasts. *ECMWF Newsletter*, 156:18–22, 2018.
- M. Chevallier, G. C. Smith, F. Dupont, J.-F. Lemieux, G. Forget, Y. Fujii, F. Hernandez, R. Msadek, K. A. Peterson, A. Storto, T. Toyoda, M. Valdivieso, G. Vernieres, H. Zuo, M. Balmaseda, Y.-S. Chang, N. Ferry, G. Garric, K. Haines, S. Keeley, R. M. Kovach, T. Kuragano, S. Masina, Y. Tang, H. Tsujino, and X. Wang. Intercomparison of the arctic sea ice cover in global ocean–sea ice reanalyses from the ora-ip project. *Climate Dynamics*, 49(3):1107–1136, Aug 2017. ISSN 1432-0894. doi: 10.1007/s00382-016-2985-y. URL <https://doi.org/10.1007/s00382-016-2985-y>.

- D. P. Dee, S. M. Uppala, A. J. Simmons, P. Berrisford, P. Poli, S. Kobayashi, U. Andrae, M. A. Balmaseda, G. Balsamo, P. Bauer, P. Bechtold, A. C. M. Beljaars, L. van de Berg, J. Bidlot, N. Bormann, C. Delsol, R. Dragani, M. Fuentes, A. J. Geer, L. Haimberger, S. B. Healy, H. Hersbach, E. V. Hólm, L. Isaksen, P. Kållberg, M. Köhler, M. Matricardi, A. P. McNally, B. M. Monge-Sanz, J.-J. Morcrette, B.-K. Park, C. Peubey, P. de Rosnay, C. Tavolato, J.-N. Thépaut, and F. Vitart. The ERA-Interim reanalysis: configuration and performance of the data assimilation system. *Quarterly Journal of the Royal Meteorological Society*, 137(656):553–597, 4 2011. ISSN 00359009. doi: 10.1002/qj.828. URL <http://doi.wiley.com/10.1002/qj.828>.
- G. Dibarboure, M.-I. Pujol, F. Briol, P. Y. L. Traon, G. Larnicol, N. Picot, F. Mertz, and M. Ablain. Jason-2 in DUACS: Updated System Description, First Tandem Results and Impact on Processing and Products. *Marine Geodesy*, 34(3-4):214–241, 2011. doi: 10.1080/01490419.2011.584826. URL <https://doi.org/10.1080/01490419.2011.584826>.
- C. J. Donlon, M. Martin, J. Stark, J. Roberts-Jones, E. Fiedler, and W. Wimmer. The Operational Sea Surface Temperature and Sea Ice Analysis (OSTIA) system. *Remote Sensing of Environment*, 116: 140–158, 2012. ISSN 00344257. doi: 10.1016/j.rse.2010.10.017.
- T. Fichefet and M. A. Maqueda. Sensitivity of a global sea ice model to the treatment of ice thermodynamics and dynamics. *Journal of Geophysical Research: Oceans*, 102(C6):12609–12646, 1997. doi: 10.1029/97JC00480.
- S. A. Good, M. J. Martin, and N. A. Rayner. EN4: Quality controlled ocean temperature and salinity profiles and monthly objective analyses with uncertainty estimates. *Journal of Geophysical Research: Oceans*, 118(12):6704–6716, 2013. ISSN 21699291. doi: 10.1002/2013JC009067.
- V. Gouretski and F. Reseghetti. On depth and temperature biases in bathythermograph data: Development of a new correction scheme based on analysis of a global ocean database. *Deep-Sea Research Part I: Oceanographic Research Papers*, 57(6):812–833, 2010. ISSN 09670637. doi: 10.1016/j.dsr.2010.03.011.
- R. L. Haney. Surface Thermal Boundary Condition for Ocean Circulation Models. *Journal of Physical Oceanography*, 1(4):241–248, 1971. doi: 10.1175/1520-0485(1971)001<0241:STBCFO>2.0.CO;2.
- H. Hersbach and D. Dee. ERA5 reanalysis is in production. *ECMWF Newsletter*, 147, 2016.
- S. Hirahara, M. A. Balmaseda, and H. Hersbach. Sea Surface Temperature and Sea Ice Concentration for ERA5. *ERA Report Series*, 26, 2016.
- J. Karvonen, J. Vainio, M. Marnela, P. Eriksson, and T. Niskanen. A Comparison Between High-Resolution EO-Based and Ice Analyst-Assigned Sea Ice Concentrations. *IEEE Journal of Selected Topics in Applied Earth Observations and Remote Sensing*, 8(4):1799–1807, apr 2015. ISSN 1939-1404. doi: 10.1109/JSTARS.2015.2426414. URL <http://ieeexplore.ieee.org/document/7105862/>.
- S. Keeley and K. Mogensen. Dynamic sea ice in the IFS. *ECMWF Newsletter*, 156:23–29, 2018.
- J. J. Kennedy, N. A. Rayner, R. O. Smith, D. E. Parker, and M. Saunby. Reassessing biases and other uncertainties in sea surface temperature observations measured in situ since 1850: 2. Biases and homogenization. *Journal of Geophysical Research*, 116(D14):D14104, 2011a. ISSN 0148-0227. doi: 10.1029/2010JD015220. URL <http://doi.wiley.com/10.1029/2010JD015220>.

- J. J. Kennedy, N. A. Rayner, R. O. Smith, D. E. Parker, and M. Saunby. Reassessing biases and other uncertainties in sea surface temperature observations measured in situ since 1850: 1. Measurement and sampling uncertainties. *Journal of Geophysical Research Atmospheres*, 116(14), 2011b. ISSN 01480227. doi: 10.1029/2010JD015218.
- R. Kwok, G. F. Cunningham, M. Wensnahan, I. Rigor, H. J. Zwally, and D. Yi. Thinning and volume loss of the Arctic Ocean sea ice cover: 20032008. *Journal of Geophysical Research*, 114(C7):C07005, 2009. ISSN 0148-0227. doi: 10.1029/2009JC005312. URL <http://doi.wiley.com/10.1029/2009JC005312>.
- W. G. Large and S. G. Yeager. The global climatology of an interannually varying air–sea flux data set. *Climate Dynamics*, 33(2-3):341–364, 2009.
- D. J. Lea, J.-P. Drecourt, K. Haines, and M. J. Martin. Ocean altimeter assimilation with observational- and model-bias correction. *Quarterly Journal of the Royal Meteorological Society*, 134(636):1761–1774, 2008.
- J. F. Legeais, M. Ablain, L. Zawadzki, H. Zuo, J. A. Johannessen, M. G. Scharffenberg, L. Fenoglio-Marc, M. Joana Fernandes, O. Baltazar Andersen, S. Rudenko, P. Cipollini, G. D. Quartly, M. Passaro, A. Cazenave, and J. Benveniste. An improved and homogeneous altimeter sea level record from the ESA Climate Change Initiative. *Earth System Science Data*, 10(1):281–301, 2018. ISSN 18663516. doi: 10.5194/essd-10-281-2018.
- G. Madec. *NEMO ocean engine*. Note du Pôle de modélisation, Institut Pierre-Simon Laplace (IPSL), France, No 27, ISSN No 1288-1619, 2008.
- S. Masina, A. Storto, N. Ferry, M. Valdivieso, K. Haines, M. Balmaseda, H. Zuo, M. Drevillon, and L. Parent. An ensemble of eddy-permitting global ocean reanalyses from the MyOcean project. *Climate Dynamics*, 49(3):813–841, 2017. ISSN 14320894. doi: 10.1007/s00382-015-2728-5.
- C. J. Merchant, O. Embury, J. Roberts-Jones, E. Fiedler, C. E. Bulgin, G. K. Corlett, S. Good, A. McLaren, N. Rayner, S. Morak-Bozzo, and C. Donlon. Sea surface temperature datasets for climate applications from Phase 1 of the European Space Agency Climate Change Initiative (SST CCI). *Geoscience Data Journal*, 1(2):179–191, 11 2014. ISSN 20496060. doi: 10.1002/gdj3.20. URL <http://doi.wiley.com/10.1002/gdj3.20>.
- C. J. Merchant, O. Embury, J. Roberts-Jones, E. K. Fiedler, C. E. Bulgin, G. Corlett, S. Good, A. McLaren, N. Rayner, and C. Donlon. ESA Sea Surface Temperature Climate Change Initiative (ESA SST CCI): Analysis long term product version 1.1. Technical report, Centre for Environmental Data Analysis, 2016. URL <http://dx.doi.org/10.5285/2262690A-B588-4704-B459-39E05527B59A>.
- K. Mogensen, M. A. Balmaseda, and A. Weaver. The NEMOVAR ocean data assimilation system as implemented in the ECMWF ocean analysis for System 4. *ECMWF Technical Memorandum*, 668: 1–59, 2012.
- T. Penduff, M. Juza, L. Brodeau, G. C. Smith, B. Barnier, J.-M. Molines, A.-M. Treguier, and G. Madec. Impact of global ocean model resolution on sea-level variability with emphasis on interannual time scales. *Ocean Science*, 6:269–284, 2010. ISSN 1812-0792. doi: 10.5194/os-6-269-2010. URL <http://archimer.ifremer.fr/doc/00003/11386/%5Cnhttp://www.ocean-sci.net/6/269/2010/>.

- P. Poli, H. Hersbach, D. P. Dee, P. Berrisford, A. J. Simmons, F. Vitart, P. Laloyaux, D. G. H. Tan, C. Peubey, J.-N. Thépaut, Y. Trémolet, E. V. Hólm, M. Bonavita, L. Isaksen, M. Fisher, P. Poli, H. Hersbach, D. P. Dee, P. Berrisford, A. J. Simmons, F. Vitart, P. Laloyaux, D. G. H. Tan, C. Peubey, J.-N. Thépaut, Y. Trémolet, E. V. Hólm, M. Bonavita, L. Isaksen, and M. Fisher. ERA-20C: An Atmospheric Reanalysis of the Twentieth Century. *Journal of Climate*, 29(11):4083–4097, 6 2016. ISSN 0894-8755. doi: 10.1175/JCLI-D-15-0556.1. URL <http://journals.ametsoc.org/doi/10.1175/JCLI-D-15-0556.1>.
- M.-I. Pujol, Y. Faugère, G. Taburet, S. Dupuy, C. Pelloquin, M. Ablain, and N. Picot. DUACS DT2014: the new multi-mission altimeter data set reprocessed over 20 years. *Ocean Science*, 12(5):1067–1090, 9 2016. ISSN 1812-0792. doi: 10.5194/os-12-1067-2016. URL <http://www.ocean-sci.net/12/1067/2016/>.
- G. D. Quartly, J. F. Legeais, M. Ablain, L. Zawadzki, M. Joana Fernandes, S. Rudenko, L. Carrère, P. Nilo Garcíá, P. Cipollini, O. B. Andersen, J. C. Poisson, S. Mbajon Njiche, A. Cazenave, and J. Benveniste. A new phase in the production of quality-controlled sea level data. *Earth System Science Data*, 9(2):557–572, 2017. ISSN 18663516. doi: 10.5194/essd-9-557-2017.
- R. W. Reynolds, T. M. Smith, C. Liu, D. B. Chelton, K. S. Casey, and M. G. Schlax. Daily high-resolution-blended analyses for sea surface temperature. *Journal of Climate*, 20(22):5473–5496, 2007.
- J. Servonnat, J. Mignot, E. Guilyardi, D. Swingedouw, R. Séférian, and S. Labetoulle. Reconstructing the subsurface ocean decadal variability using surface nudging in a perfect model framework. *Climate Dynamics*, 44(1-2):315–338, 2014. ISSN 14320894. doi: 10.1007/s00382-014-2184-7.
- A. Sørensen and T. Lavergne. Sea Ice Climate Change Initiative : D3.4 Product User Guide (PUG). Technical report, Norwegian Meteorological Institute, February 2017. URL <http://www.esa-seaice-cci.org>.
- T. Stockdale, S. Johnson, L. Ferranti, M. A. Balmaseda, and S. Briceag. ECMWF’s new long-range forecasting system SEAS5. *ECMWF Newsletter*, 154:15–20, 2017.
- S. Tietsche, M. A. Balmaseda, H. Zuo, and K. Mogensen. Arctic sea ice in the global eddy-permitting ocean reanalysis ORAP5. *Climate Dynamics*, pages 1–15, 6 2015. ISSN 0930-7575. doi: 10.1007/s00382-015-2673-3. URL <http://link.springer.com/10.1007/s00382-015-2673-3>.
- S. Tietsche, M. Alonso-Balmaseda, P. Rosnay, H. Zuo, X. Tian-Kunze, and L. Kaleschke. Thin arctic sea ice in l-band observations and an ocean reanalysis. *The Cryosphere*, 12(6):2051–2072, 2018. doi: 10.5194/tc-12-2051-2018. URL <https://www.the-cryosphere.net/12/2051/2018/>.
- H. A. Titchner and N. A. Rayner. The Met Office Hadley Centre sea ice and sea surface temperature data set, version 2: 1. Sea ice concentrations. *Journal of Geophysical Research: Atmospheres*, 119: 2864–2889, 2014. ISSN 2169897X. doi: 10.1002/2013JD020316. URL <http://doi.wiley.com/10.1002/2013JD020316>.
- P. Uotila, H. Goosse, K. Haines, M. Chevallier, A. Barthélemy, C. Bricaud, J. Carton, N. Fučkar, G. Garric, D. Iovino, F. Kauker, M. Korhonen, V. S. Lien, M. Marnela, F. Massonnet, D. Mignac, K. A. Peterson, R. Sadikni, L. Shi, S. Tietsche, T. Toyoda, J. Xie, and Z. Zhang. An assessment of ten ocean reanalyses in the polar regions. *Climate Dynamics*, May 2018. ISSN 1432-0894. doi: 10.1007/s00382-018-4242-z. URL <https://doi.org/10.1007/s00382-018-4242-z>.

- S. M. Uppala, P. W. Kållberg, A. J. Simmons, U. Andrae, V. D. C. Bechtold, M. Fiorino, J. K. Gibson, J. Haseler, A. Hernandez, G. A. Kelly, X. Li, K. Onogi, S. Saarinen, N. Sokka, R. P. Allan, E. Andersson, K. Arpe, M. A. Balmaseda, A. C. M. Beljaars, L. V. D. Berg, J. Bidlot, N. Bormann, S. Caires, F. Chevallier, A. Dethof, M. Dragosavac, M. Fisher, M. Fuentes, S. Hagemann, E. Hólm, B. J. Hoskins, L. Isaksen, P. a. E. M. Janssen, R. Jenne, A. P. McNally, J.-F. Mahfouf, J.-J. Morcrette, N. A. Rayner, R. W. Saunders, P. Simon, A. Sterl, K. E. Trenberth, A. Untch, D. Vasiljevic, P. Viterbo, and J. Woollen. The ERA-40 re-analysis. *Quarterly Journal of the Royal Meteorological Society*, 131(612):29613012, 2005. ISSN 1477-870X. doi: 10.1256/qj.04.176.
- A. T. Weaver, C. Deltel, . Machu, S. Ricci, and N. Daget. A multivariate balance operator for variational ocean data assimilation. *Quarterly Journal of the Royal Meteorological Society*, 131(613):3605–3625, 2005.
- S. E. Wijffels, J. Willis, C. M. Domingues, P. Barker, N. J. White, A. Gronell, K. Ridgway, and J. A. Church. Changing expendable bathythermograph fall rates and their impact on estimates of thermohaline sea level rise. *Journal of Climate*, 21(21):5657–5672, 2008.
- H. Zuo, M. A. Balmaseda, and K. Mogensen. The ECMWF-MyOcean2 eddy-permitting ocean and sea-ice reanalysis ORAP5. Part 1: Implementation. *ECMWF Technical Memorandum*, 736, 2015.
- H. Zuo, M. A. Balmaseda, E. D. Boisseson, S. Hirahara, M. Chrust, and P. D. Rosnay. A generic ensemble generation scheme for data assimilation and ocean analysis. *ECMWF Technical Memorandum*, 795, 2017a.
- H. Zuo, M. A. Balmaseda, and K. Mogensen. The new eddy-permitting ORAP5 ocean reanalysis: description, evaluation and uncertainties in climate signals. *Climate Dynamics*, 49(3):791–811, aug 2017b. ISSN 1432-0894. doi: 10.1007/s00382-015-2675-1. URL <https://doi.org/10.1007/s00382-015-2675-1>.
- H. Zuo, L. Vidar, A. B. Sandø, G. Garric, C. Bricaud, A. Storto, K. A. Peterson, S. Tietsche, and M. Mayer. Copernicus Marine Monitoring Service Ocean State: Extreme sea-ice conditions. *Journal of Operational Oceanography*, *accepted*, 2018.